NATIONAL ADVISORY COMMITTEE FOR AERONAUTICS

TECHNICAL NOTE

No. 1807

EFFECTS OF PARTIAL ADMISSION ON PERFORMANCE OF A GAS TURBINE

By Robert C. Kohl, Howard Z. Herzig
and Warren J. Whitney

Lewis Flight Propulsion Laboratory
Cleveland, Ohio

Washington
February 1949

NATIONAL ADVISORY COMMITTEE FOR AERONAUTICS

TECHNICAL NOTE No. 1807

EFFECTS OF PARTIAL ADMISSION ON PERFORMANCE OF A GAS TURBINE

By Robert C. Kohl, Howard Z. Herzig
and Warren J. Whitney

SUMMARY

The effects of partial admission of the driving fluid on the performance of a representative full-admission, production-type gas turbine were investigated.

In successive studies, the turbine was operated with full (360°) peripheral admission and with admission confined to 120° and 180° of the nozzle annulus. The corrected power output and over-all efficiency for these configurations are compared. Significance of the turbine losses is considered and the types and amounts of loss encountered with full and partial admission are tabulated. The occurrence of turbine-blade vibration induced by fractional-arc admission is discussed.

Methods are presented for prediction of over-all turbine efficiency and power output for any degree of partial admission. These predictions of power output are accurate within ±1 percent of corresponding observed values over most of the speed range and within ±3 percent at the highest speeds. Efficiency predictions are within 1 point over most of the speed range and within $\pm 1\frac{1}{2}$ points at the lower and higher ends of the speed range. These predictions indicate marked losses in efficiency at admission of less than 180°.

INTRODUCTION

As applied to turbines, the term "partial admission" refers to a configuration in which the driving fluid is admitted to only a fraction of the nozzle annulus. Partial admission has long been used in steam-turbine practice; however, little application of this technique is known to have been made to gas turbines that have relatively high pressure ratios per stage. Partial admission is one of the possible methods that could be used for obtaining

part-load operation or power regulation. This method could utilize a system of individual gas generators, each generator discharging into a section of the turbine-nozzle periphery, the number of generators fired depending on the general turbine power output desired.

An analytical study of the manner in which normal turbine operating losses arise was made at the NACA Lewis laboratory and is presented herein. The additional losses introduced by use of partial admission are also discussed. This study further shows that the turbine performance at full and partial admission can be correlated on the basis of the loss differentials.

In order to determine quantitatively the effect of partial admission on turbine power output and turbine efficiency, a representative single-stage turbine was modified to restrict the driving fluid to 120° and 180° of the nozzle annulus. At 120° admission, turbine performance was obtained for three values of total-pressure ratio, a range of nozzle-inlet pressures from 20 to 45 inches of mercury absolute, an inlet temperature of 800° R, and over a range of rotor speeds that includes the design rotor speed as corrected to standard conditions. At 180° admission, turbine performance was obtained at a total-pressure ratio of 2.0, an inlet total pressure of 45 inches of mercury absolute, and an inlet temperature of 800° R over the complete range of corrected rotor speeds. Performance with full and partial admission at equivalent operating conditions is compared on the basis of corrected power output and over-all efficiencies. Because no provision was made for motoring the turbine, rotational losses were calculated using applicable loss formulas. Validity of these formulas was established by using actual loss measurements on a smaller, though similar, turbine.

Partial admission is considered as a power-reduction device. The methods developed for estimating the losses were used to make a study of the effects of partial admission at various degrees of admission; the results of the study are summarized in a curve of power reduction plotted against efficiency. This curve is then superimposed on composite-type plots representing the individual effects of the normally interacting turbine operating variables. The procedure permits ready comparison of partial admission as a method of power reduction with other methods such as, inlet pressure, pressure ratio, and rotor speed on the basis of flexibility, range of effectiveness, and over-all efficiency at reduced power levels.

The causes of induced turbine-rotor-blade vibration are briefly discussed and means are examined for minimizing the effect of vibrational stresses at resonance conditions.

ANALYSIS

The ideal power in the driving fluid of any turbine may be expressed by

$$\text{ideal power} = W\Delta_g h' \tag{1}$$

where

W weight flow through turbine

$\Delta_g h'$ isentropic enthalpy drop per pound of driving fluid based on total-pressure ratio

Primed symbols indicate stagnation state. (All symbols used in this analysis are defined in appendix A.)

Use of the isentropic enthalpy drop based on total-pressure ratio assumes that useful work can be recovered from the turbine-discharge gas velocity.

Not all the weight flow expressed in equation (1) is available to the turbine for doing work. Some fraction of the gas flow passes through the clearance space between the rotor-blade tips and the stationary turbine outer casing. The presence of this rotor-tip leakage constitutes a turbine power loss. Friction, separation, and other viscous effects give rise to losses in the nozzle and rotor flow passages, which further prevent realization of the ideal power in equation (1).

Gross power is defined as ideal power minus these rotor-tip leakage and nozzle and rotor-blading losses.

The mechanism by which power is derived from the driving fluid in a turbine is described by

$$\text{blade power} = W(1-K_I)\, u_m(\bar{c}_{u,1}-\bar{c}_{u,2}) \tag{2}$$

where

K_I percentage of active gas through rotor-tip clearance space, constant for any particular turbine

u velocity, (ft/sec)

c absolute velocity, (ft/sec)

Subscripts m, u, 1, and 2 refer to pitch line, tangential, rotor inlet, and rotor discharge, respectively. Barred symbols refer to average values.

Blade power and gross power are the same for a full-admission turbine. They are different, however, for a turbine operating with partial admission as will be subsequently shown.

A part of the blade power produced is so dissipated by shaft losses that the available net power for a full-admission turbine may be written

$$\begin{aligned}\text{net power} = {} & \text{ideal power} - \text{rotor-tip leakage losses} \\ & - \text{aerodynamic nozzle and rotor-blading losses} \\ & - \text{shaft losses}\end{aligned} \tag{3}$$

Blade power can be described by

$$\text{blade power} = \text{net power} + \text{shaft losses} \tag{4}$$

Summarized in schematic form in figure 1(a) are the relations between the various concepts of turbine power for full admission.

For greater utility, the performance data are presented as corrected to a constant reference state. The reference state commonly chosen and used herein is standard sea-level conditions.

At constant Mach number

$$\frac{V}{a} = \frac{V}{\sqrt{\gamma g R T}} = \frac{V_0}{a_0} = \frac{V_0}{\sqrt{\gamma g R T_0}} \tag{5}$$

where

V any gas velocity term observed, (ft/sec)

a velocity of sound at observed conditions, (ft/sec)

γ ratio of specific heats of gas

g acceleration due to gravity, 32.174, (ft/sec^2)

R gas constant, 53.345, (ft-lb)/(lb)($^\circ$F)

T temperature observed, ($^\circ$R)

The subscript 0 refers to corrected conditions at NACA sea level in each case.

Therefore

$$V_0 = \frac{V}{\sqrt{\theta}} \tag{6}$$

where θ is the temperature correction ratio, T/T_0.

$$\rho_0 = \rho \frac{\theta}{\delta} \tag{7}$$

where

ρ mass density, (slugs/cu ft)

δ pressure correction ratio, p/p_0

p absolute pressure, (lb/sq ft) or (in. Hg)

$$W_0 = \frac{W\sqrt{\theta}}{\delta} \tag{8}$$

$$\Delta_s h_0' = \frac{\Delta_s h'}{\theta} \tag{9}$$

$$(\text{power})_0 = \frac{(\text{power})}{\delta\sqrt{\theta}} \tag{10}$$

Correction of any performance or loss expression can be made by correcting the terms within that expression which are variable with changes in altitude, as indicated in equations (5) to (10).

If the pressure relations throughout the turbine are maintained constant, the correction of performance or loss expressions to equivalent sea-level values may be made by using correction factors based on the gas properties at some convenient reference point in the turbine. The reference point selected is the turbine inlet. That the performance or loss expression may contain terms involving gas properties at locations other than at the reference point does not alter the validity of the procedure for it can be shown that changes of temperature, pressure, and Mach number at the reference point are generally reflected by similar changes throughout the turbine in most practical applications.

Full-Admission Turbine Performance

In the case of a turbine operating with full-peripheral admission, the ideal power output corrected to sea level is expressed as

$$(\text{ideal power})_0 = \frac{W\Delta_s h'}{\delta_i\sqrt{\theta_i}} \tag{11}$$

where subscript i refers to the conditions at the inlet measuring station.

Losses. - The principle turbine losses with full admission that must be subtracted from the ideal power are:

1. rotor-tip leakage loss

2. nozzle and rotor-blading aerodynamic losses

3. shaft losses, which for a full-admission turbine include

   (a) disk-windage loss

   (b) bearing loss

(1) Rotor-tip leakage loss: The percentage of active gas flow that passes over the rotor-blade tips may be estimated by the following expression as indicated in references 1 and 2:

percentage of active gas flow through tip clearance space

$$= \frac{100\ C}{nl\ \sin\beta_2 + C} \tag{12}$$
$$= K_I$$

where

C blade radial tip clearance, (ft)

n thickness coefficient (unity for reaction turbines)

l rotor-blade length, (ft)

β_2 rotor-blade exit angle relative to plane of rotor disk measured at pitch line, (deg)

The leakage power loss is taken as the product of the leakage gas weight flow and the isentropic enthalpy drop based on the total-pressure ratio across the turbine. The leakage loss was calculated by the expression

$$\text{leakage loss} = K_I W \Delta_s h' \tag{13}$$

In order to correct to sea-level conditions, the loss, as obtained by the preceding expression, is multiplied by the factor $\frac{1}{\delta_i \sqrt{\theta_i}}$.

(2) Nozzle and rotor-blading aerodynamic losses: Friction, separation, and other viscous effects result in losses as they affect the gas-velocity components in equation (2) in any operating passage. In this investigation these losses are not directly determined.

(3) Shaft losses:

(a) Disk-windage loss. The disk-windage (disk-friction) loss was taken as the power required to rotate the rotor disk, without blades, against the frictional drag of the relatively stagnant gases in the clearance space on each side of the rotor disk. This power loss may be represented by the following expression adapted from equation [7] of reference 3:

$$\text{disk power loss} = K_{II}\left(\frac{\rho_d d_h u_h}{\mu_d}\right)^{-0.12}\left(\frac{N}{1000}\right)^3 d_h^5 \rho_d \tag{14}$$

where

K_{II} empirical constant for disk-windage loss to be determined for a particular turbine by tests

d rotor-disk diameter, (ft)

μ absolute viscosity, ((lb)(sec)/sq ft)

N rotational speed, (rpm)

Subscripts h and d refer to the blade-root position and the fluid surrounding the turbine-rotor disk, respectively.

By use of equations (5) to (10) and the relation $\left(\frac{\mu_i}{\mu_0}\right) \sim \left(\frac{T_i'}{T_0'}\right)^{0.6}$, which is valid for the range of temperatures normally encountered in turbine operation, the power loss as corrected to standard sea-level conditions may be written as

$$\text{power loss} = K_{II}\left(\frac{\rho_d d_h u_h}{\mu_d}\right)^{-0.12} \left(\frac{N}{1000}\right)^3 d_h^5 \rho_d \frac{1}{\delta_i^{0.88}\theta_i^{0.632}} \quad (15)$$

(b) Bearing loss. It was assumed that the entire frictional loss of the bearings appeared as the observed temperature rise of the lubricating oil.

$$\text{bearing power loss} = W_{oil}\, c_{p,oil}\, \Delta T_{oil} \quad (16)$$

where

c_p specific heat at constant pressure, Btu/(lb)($^\circ$F)

ΔT_{oil} temperature rise of lubricating oil in bearings, $^\circ$F

This power loss was considered to be constant at any altitude (and degree admission); therefore, no correction factor is used.

Turbine over-all efficiency. - The over-all efficiency of a turbine may be defined as

$$\eta' = \frac{\text{net power}}{\text{ideal power}} \quad (17)$$

where η' is the efficiency based on total-pressure ratio.

Partial-Admission Turbine Performance

The ideal power in the driving fluid of any turbine operating with partial admission may be expressed by

$$(\text{ideal power})_F = W_F\, \Delta_s h' \quad (18)$$

where the subscript F refers to partial admission.

A basic assumption made in the estimation of turbine performance at various degrees of admission is that the weight flow of

driving fluid is directly proportional to the number of active nozzle passages, that is, to the fraction of active nozzle arc. (Data obtained at partial admission bear this out experimentally.)

Of the major turbine losses that occur with full peripheral admission, the rotor-tip leakage loss and the nozzle and rotor-blading aerodynamic losses as defined are proportional to the number of active nozzle passages; whereas the shaft losses are independent of the degree of admission.

Then, under fixed conditions of inlet-gas total temperature, inlet total pressure, total-pressure ratio across the turbine wheel, and rotative speed of the wheel, the gross power output with no losses must be proportional to the weight flow and hence to the degree of admission.

$$(\text{gross power})_F = F\ (\text{gross power})_{360^\circ} \tag{19}$$

where F is a fraction of the active nozzle arc and the subscript 360° refers to full admission.

Losses. - A turbine operating with partial admission is subject to certain inherent losses in addition to the normal losses encountered in a full-admission turbine.

Additional losses encountered with partial admission include:

(1) pumping or windage loss in inactive rotor blading

(2) driving-fluid losses, which include

  (a) scavenge and eddy losses during filling and emptying of rotor blading

  (b) loss due to diffusion of gases at nozzle discharge (primarily encountered in reaction-type machines)

For these studies the scavenge, eddy, and diffusion losses have been combined and considered in the aggregate as driving-fluid losses.

Correlation of data for runs with different degrees of admission requires a quantitative statement of these combined losses, the refinement of the correlation being dependent on the accuracy and the comprehensiveness of the survey of these quantities.

(1) Pumping loss: Pumping, windage, or fanning loss is caused by the induced circulation of the nonworking gases in the inactive rotor passages. The expression that is used to estimate this loss is similar to the general form listed in reference 4, (equation (7), p. 201) and states that

$$\text{pumping power loss} = \lambda\left(\frac{l}{D}\right) D^5\left(\frac{N}{1000}\right)^3(1-F)\rho_d \tag{20}$$

where

λ empirical constant, depending upon inactive blade shrouding

D pitch-line diameter, (ft)

When the expression for pumping power loss is corrected for sea-level conditions the equation is

$$\text{pumping power loss} = \lambda\left(\frac{l}{D}\right) D^5\left(\frac{N}{1000}\right)^3\rho_d(1-F)\frac{1}{\delta_i\sqrt{\theta_1}} \tag{21}$$

(2) Driving fluid loss: The power produced by the blading of a full-admission turbine may be expressed as

$$\text{blade power} = W\frac{\pi DN}{60}\left[(\bar{c}_{u,1})_{360^\circ} - (\bar{c}_{u,2})_{360^\circ}\right] \tag{22}$$

This expression may be written as

$$\text{blade power per blade} = K_{III}\sum_{r_h}^{r_T}\bar{\rho}_i\, N(c_{x,1})_{360^\circ}\left[(c_{u,1})_{360^\circ} - (c_{u,2})_{360^\circ}\right] \tag{23}$$

where

$$K_{III} = \frac{\pi^2 D^2 l}{60 b}\frac{\bar{\rho}_1}{\bar{\rho}_i}$$

K_{III} empirical constant for driving-fluid losses to be determined for particular turbine

r radius, (ft)

b total number of rotor blades

The subscripts x, h, and T refer to axial, inner-radius (blade root) position, and outer-radius position, respectively.

As unbarred symbols, $(c_{x,1})_{360^o}$, $(c_{u,1})_{360^o}$, and $(c_{u,2})_{360^o}$ represent the velocities of the gases at any blade height from root r_h to tip r_T. Included in constant K_{III} is $\frac{\bar{\rho}_1}{\bar{\rho}_i}$, which was found to be essentially constant over the speed range.

Therefore, the blade power output of a turbine at full admission may be found by summing up the individual powers developed by all the blades.

$$(\text{blade power})_{360^o}$$

$$= K_{III} \sum_{B=0}^{B=b} \sum_{r_h}^{r_T} \bar{\rho}_i \, N(c_{x,1})_{360^o} \left[(c_{u,1})_{360^o} - (c_{u,2})_{360^o}\right] \qquad (24)$$

where B is the number of active rotor blades at any instant.

Losses occur as the result of the scavenging action that must take place as a previously inactive rotor passage enters the active arc of one rotational cycle. The relatively stagnant gases entrapped in the passage during the inactive arc of the cycle are displaced by the recurring active fluid flow. This displacement process requires a rapid acceleration of the displaced gases and a concurrent mixing with the displacing gases that occasion a momentum loss.

At the completion of the active arc of the cycle, the reverse occurs and is accompanied by the formation of eddies as the active flow through the channels is reduced and finally cut off entirely.

The losses with partial admission resulting from the mixing of active and stagnant gases are manifested as changes in the

velocity components of the driving gases through the turbine rotor and represent unavailable power in the driving fluid.

An additional loss may be introduced in a reaction-type turbine in which there is a tendency for some of the driving fluid to diffuse at the nozzle discharge and to spread throughout the clearance space between the nozzles and the rotor blading. The subsequent loss results chiefly from the unfavorable rotor-inlet velocity component of these diffused gases.

Each of these losses has a common characteristic, which permits them to be grouped into a single aggregate loss. The relating characteristic is that the magnitude of each loss is a function of the product of the gas density and the rotor speed to the first power.

$$\left.\begin{array}{l}\text{scavenging loss}\\ \text{eddy loss}\\ \text{diffusion loss}\end{array}\right\} \sim f(K_{III}\bar{\rho}_i N)$$

These losses in the driving fluid itself, which have been designated driving-fluid losses, are thus distinguished from the shaft and tip leakage losses in the text. Driving-fluid losses are not reliably or readily evaluated from gas-state measurements because of the mixing action of the gases that produces them. Accordingly, they must be experimentally determined and compared with a general expression developed to describe them, as follows:

Gross power and blade power are seen to be related by the equation

$$\text{gross power} = \text{blade power} + \text{driving-fluid losses} \qquad (25)$$

Because at 360° admission there are no significant driving-fluid losses, the driving-fluid losses can be determined from equations (19) and (25) as

$$(\text{driving-fluid losses})_F = F\,(\text{blade power})_{360^\circ} - (\text{blade power})_F \qquad (26)$$

Use of power expressions corrected to sea-level conditions results in evaluation of driving-fluid losses corrected to sea-level conditions.

This equation is used to evaluate the driving-fluid losses due to partial admission. The driving-fluid losses represent the amount by which the blade power output at partial admission fails to equal the fraction of full-admission power represented by the admission ratio.

A more general expression that defines the driving-fluid losses may be developed. From equations (24) and (26),

$$(\text{driving-fluid losses})_F$$

$$= FK_{III}\bar{\rho}_i N \left\{ \sum_{B=0}^{B=b} \sum_{r_h}^{r_T} (c_{x,1})_{360^\circ} \left[(c_{u,1})_{360^\circ} - (c_{u,2})_{360^\circ} \right] \right\}$$

$$- K_{III}\bar{\rho}_i N \left\{ \sum_{B=0}^{B=bF} \sum_{r_h}^{r_T} (c_{x,1})_F \left[(c_{u,1})_F - (c_{u,2})_F \right] \right\} \qquad (27)$$

where the number of active blades at any instant B equals Fb and $(c_{x,1})_F$, $(c_{u,1})_F$, and $(c_{u,2})_F$ are the gas velocities that are present at that degree of admission.

Equation (27) expresses the differential between the power output with nozzle-arc reduction as would be indicated on the basis of reduced weight flow and the actual power output as would be observed for that same amount of nozzle-arc reduction. For fixed conditions of gas state and rotor speed, good correlation is obtained if this power difference is considered to increase linearly with the amount of active nozzle reduction over the range of practical reductions.

$$\frac{(\text{driving-fluid losses})_F}{(\text{driving-fluid losses})_G} = \frac{1-F}{1-G} \qquad (28)$$

where F and G are the fractions of active nozzle arc for any particular degrees of admission.

The net observed dynamometer power at partial admission must now be written

$$(\text{net power})_F = (\text{ideal power})_F - (\text{rotor-tip leakage loss})_F - (\text{nozzle and rotor-blading losses})_F - (\text{shaft losses})_F - (\text{driving-fluid losses})_F \quad (29)$$

This equation corresponds to equation (3) for full-admission turbines.

From the preceding discussion,

$$(\text{net power})_F = F(\text{gross power})_{360^\circ} - (\text{shaft losses})_F - (\text{driving-fluid losses})_F \quad (30)$$

Power and efficiency estimation. - Equation (30) indicates a procedure for estimating turbine power output at any degree of admission from the turbine output with full admission once the driving-fluid losses have been determined.

Over-all efficiency for a turbine operating with partial admission then, is calculated,

$$\eta' = \frac{(\text{net power})_F}{(\text{ideal power})_F} \quad (31)$$

Efficiency estimations are based on the assumption that the ratio of the efficiencies of any two degrees of admission is proportional to the ratio of the observed powers per pound of driving fluid developed at these admissions. The equation

$$\frac{\eta'_F}{\eta'_{360^\circ}} = \frac{\left(\frac{P_F}{W_F}\right)}{\left(\frac{P_{360^\circ}}{W_{360^\circ}}\right)} \quad (32)$$

compares the efficiency for partial admission with full-admission data.

Because, as previously discussed, the weight flow is assumed proportional to the degree of admission, equation (32) becomes

$$\eta'_F = \frac{1}{F}\left(\frac{P_F}{P_{360^\circ}}\right)\eta'_{360^\circ} \tag{33}$$

Power-Control Parameters

For a given turbine, power is a function of the independent variables as stated by

$$\text{power} = f\left(Re_i, M_i, \gamma, p_i', \frac{p_i'}{p_e'}, N, T_i', F\right) \tag{34}$$

where

Re Reynolds number

M Mach number

and the subscript e refers to turbine discharge.

Of these parameters, turbine-inlet pressure, turbine pressure ratio, rotor speed, turbine-inlet temperature, and combinations of any two or more of these variables can be used for power control. It is of interest to compare the turbine performance using partial admission as a power control with the turbine performance obtained by using these other parameters to achieve power reduction.

The individual effects of the normally interacting turbine operating variables may be isolated by allowing these independent parameters to vary one at a time while maintaining the other parameters constant. These methods of power control may then be compared with partial admissions.

EQUIPMENT

Turbine

For this investigation, the turbine used was obtained from a commercial-type jet-propulsion engine. The turbine components are the turbine-rotor assembly with bearings and bearing supports, the turbine-nozzle assembly and stationary shroud, and the combustion-chamber casing with fuel-nozzle ring.

The turbine rotor (fig. 2) has 54 tapered blades $2\frac{1}{8}$ inches long and has an over-all diameter of $16\frac{1}{8}$ inches. The turbine is equipped with reaction-type blading; the amount of reaction, however, is slight. The turbine-nozzle assembly consists of 48 nozzle blades with a height of $2\frac{1}{8}$ inches. The nozzle blades are held in position by an inner and an outer shroud band. The nozzle blades are precision cast and the rotor blades are machined. The surface finishes of each conform to the general standards for the particular methods of fabrication. Details of the rotor and nozzle blades are shown in figure 3.

Provision was made to install gas baffles in the nozzle section to effect partial admission. Two views of the arrangement with 120° active nozzle arc are shown in figure 4.

The nozzle ring, having 48 nozzle blades, allows positioning of baffle segments so that for active nozzle-arc reduction in $7\frac{1}{2}^{\circ}$ increments, a number of whole nozzle passages is active. Thus the beginning and the cut-off of admission always occur along leading edges of, rather than between, nozzle blades. (See fig. 5.)

Setup

The over-all test setup used for the investigation is shown in figure 6. Pressurized air supplied by the laboratory combustion-air system was introduced into an external hot-gas producer into which 62-octane gasoline was injected and burned. The combustion products provided the driving fluid, which then entered the turbine assembly normal to the turbine axis and flowed into the nozzle approach section in which a honeycomb-type flow straightener was installed. During this investigation, the engine burner lining was removed from the nozzle approach section and no burning was conducted at this location.

From the nozzle approach section, the driving gases then passed through the nozzles and the turbine rotor and into the discharge section. The turbine-discharge section consists of an outer cylindrical shell with an internal diameter the same as that of the turbine-wheel stationary shroud, and an inner conical piece 30 inches long, which has a base diameter the same as the root diameter of the turbine wheel. Turbine back pressures were set by throttling to the laboratory low-pressure exhaust system.

The power produced by the turbine was absorbed by an eddy-current-type absorption dynamometer (fig. 6).

Measuring Apparatus

Weight-flow measurements. - A standard A.S.M.E. flat-plate submerged orifice in the 12-inch combustion-air duct upstream of the hot-gas producer was used to measure the air flow. A calibrated rotameter was used to measure the quantity of fuel burned to heat the inlet air in the external hot-gas producer.

The turbine instrumentation used for these studies is shown in figure 7.

Nozzle-inlet section. - Four quadruple-shielded chromel-alumel thermocouples were equally spaced around the annular nozzle approach section 6 inches in front of the nozzle section to measure the turbine-inlet total temperatures. These thermocouples were sufficiently removed from the flame region to avoid radiation effects.

Four static-pressure taps in the outer shell of the combustion chamber in the same cross-sectional plane as the inlet-temperature thermocouples measured the turbine-inlet static pressures. An arithmetic average of these readings was taken as the inlet static pressure. For the runs with reduced nozzle arc, only the static-pressure taps directly upstream of the active nozzles were used.

A total-pressure probe located in the nozzle approach section about 2 inches upstream of the active nozzles was used to set inlet total pressures during turbine operation.

No instrumentation was installed in the flow region between the nozzles and the rotor blading.

Turbine-rotor section. - A thermocouple and static-pressure tap each were located in the space on both sides of the disk in order to obtain measurements used to calculate the density of the gases surrounding the rotor disk. These observed quantities were considered representative of the stagnation conditions of the gases in these locations. This instrumentation was installed only for the runs with 120° admission and the data obtained were applied to the full-admission runs. Little change of the gas state at these locations is likely to occur because of varying the amount of gas admission.

Turbine-discharge section. - Six static-pressure taps located in the plane normal to the turbine axis, $2\frac{1}{4}$ inches downstream of the discharge side of the rotor wheel, indicated the discharge static pressures. Three of the taps were installed in the outer cylindrical wall at 120° intervals and three in the inner conical piece at the same angular positions as the outer wall taps. For the runs with reduced nozzle arc, only the static-pressure taps directly downstream of the active nozzles were used.

Tail-cone discharge section. - Instrumentation was installed at the downstream end of the tail cone in an effort to establish the turbine-outlet static and total gas states after final mixing of the discharge driving fluid with the inactive gases downstream of the blocked nozzles. Two thermocouple probes, two total-pressure tubes, and three static-pressure taps spaced at 120° intervals were located as shown in figure 7. The measurements obtained, however, indicated that the mixing of the outlet gases was incomplete at this station.

Miscellaneous instrumentation. - Thermocouples to measure the temperature rise of the oil across the journal and journal-thrust bearings were installed in the oil passages into and out of the bearings.

The rate of lubricant flow was not measured during turbine operation. However, a mock-up of the lubricating system was later set up to obtain this flow rate. This mock-up consisted of the shaft and bearing assembly together with the supply and scavenge pumps and a rotameter installed in the oil-supply line.

A chronometric tachometer, driven by an electric generator geared to the dynamometer-rotor shaft was used for measuring turbine rotational speeds.

An NACA balanced-diaphragm dynamometer-torque indicator (reference 5) was used for torque measurements.

OPERATIONAL PROCEDURE

Performance

For this investigation, the inlet total temperature was maintained constant at 800° R during operation with both full and reduced admission. The range of the variable operating conditions over which data were obtained includes inlet total pressure,

total-pressure ratio, and rotor speed. With the inlet total pressure set and maintained constant, the rotor speed was varied over the entire range for each pressure ratio. This procedure was repeated for each of the range-of-inlet pressure runs. The following table gives the range of performance investigation:

Gas admission (deg)	Total-pressure ratio	Inlet total pressure (in. Hg abs.)	Corrected rotor speed, rpm[a]	
			Minimum	Maximum
360	1.50	20	3391	[b]9,227
		30	3410	12,941
		40	3354	12,925
		45	3377	12,685
	2.00	20	3484	13,128
		30	3382	13,036
		40	3611	13,100
		45	3534	12,979
	2.40	20	3463	13,157
		30	3444	13,643
		40	5292	13,304
		45	3562	12,905
120	1.50	20	3427	[b]8,921
		30	3431	[b]10,239
		45	3411	[b]10,749
	2.00	[c]20	3450	[b]10,493
		30	3412	[b]11,034
		45	3414	12,560
	2.40	20	3397	[b]10,675
		30	3436	12,185
		45	3445	12,620
180	2.00	45	3394	12,134

[a]Tip speed in feet per second equals rpm times 0.0704.
[b]Speed limited by minimum dynamometer drag.
[c]Some scatter in data.

Losses

Disk-spread friction and blade windage. - Selection of the working equations for the disk-friction and blade-windage losses was made on the basis of a comparison of the values for these losses as obtained by representative formulas with actual loss data on a smaller unit.

The principal source of measured loss data was an 11-inch-diameter gas turbine. In order to obtain loss measurements, a dynamometer was used to motor this turbine rotor, with blading attached, in a stagnant medium.

After machining off the blading to the root diameter, the rotor was motored again. Motoring was performed over a range of speeds for several values of gas density in the rotor housing. Bearing and gear losses were isolated by extrapolating the observed loss data to zero density.

Bearing loss. - A calibration of the mock-up of the lubricating system was made from which the flow rate to the journal-thrust and journal bearings could be determined over a wide range of operating oil temperatures and pressures. No turbine-shaft rotation was provided during this calibration.

Weight-Flow Check

Weight-flow measurements were made with the wheel removed at various degrees of admission. Partial admission was accomplished by blocking off fractions of the nozzle periphery. The inlet temperature was maintained at 800° R, the inlet pressures were varied over the same range as during the performance investigation with the back pressure reduced sufficiently to assure choking in the nozzles. This investigation confirmed that weight flow is directly proportional to the degree of admission.

METHODS

Calculation Methods

Full-admission performance. - Inlet total pressure was calculated on a continuity basis using the inlet static-pressure and total-temperature observations.

$$p_i' = p_i \left[\frac{1}{2} + \sqrt{\frac{1}{4} + \frac{1}{2g}\left(\frac{\gamma-1}{\gamma}\right)\left(\frac{W}{p_i A}\right)^2 RT_i'} \right]^{\frac{\gamma}{\gamma-1}} \tag{35}$$

where A is the discharge-annulus area in square feet.

The discharge total pressure was obtained by computing the axial component of the velocity of the discharge gases using

equation (9) of reference 6 and adding the corresponding velocity pressure to the measured discharge static pressure. The equation so obtained for calculating discharge total pressure is

$$p_e' = p_e \left[\frac{1}{2} + \sqrt{\frac{1}{4} + \frac{1}{2g}\left(\frac{\gamma-1}{\gamma}\right)\left(RT_i' - \frac{\gamma-1}{\gamma}\frac{P}{W}\right)\left(\frac{W}{p_e A_e}\right)^2} \right]^{\frac{\gamma}{\gamma-1}} \qquad (36)$$

The ideal power input can then be calculated from equation (1), which becomes

$$\text{ideal power} = Wc_p T_i' \left[1 - \left(\frac{p_e'}{p_i'}\right)^{\frac{\gamma-1}{\gamma}} \right] \qquad (37)$$

The turbine efficiency for the full-peripheral admission runs was taken as the ratio of the measured turbine power output to the calculated ideal power.

Because the pressure ratio across the turbine was regulated by setting the inlet total pressure and the discharge static pressure, there was some deviation in total-pressure ratio due to the variation of discharge total pressure with turbine power extraction. For comparison, it is therefore necessary to correct the turbine power output for this deviation from the nominal total-pressure ratio. The correction factor employed is the ratio of the isentropic enthalpy drop based on the nominal total-pressure ratio to the corresponding drop based on the actual total-pressure ratio.

Partial-admission performance. - Performance calculations for the runs with partial admission were similar to those for full admission. However, in computing the axial component of the discharge velocity, it was assumed that the active flow area at the discharge measuring station immediately downstream of the rotor was proportional to the amount of active nozzle arc. The observations previously mentioned, which were made at the measuring station in the plane at the tip of the tail cone, indicate that the rate of gas diffusion in the discharge section is not rapid and would serve to validate the assumption.

Rotor-tip leakage loss. - Leakage loss was taken as the energy contained in the active gas that passes through the clearance space between the rotor-blade tips and the stationary turbine outer casing. The percentage of leakage weight flow was calculated using equation (12).

For this turbine,

$$C = 0.0046 \text{ foot}$$

$$l = 0.177 \text{ foot}$$

$$\beta_2 = 40.1^\circ$$

The leakage weight flow is then 3.86 percent (K_I) of the total weight flow.

Substituting this value of K_I into equation (13) and correcting to sea-level conditions gives

$$\text{leakage loss} = \frac{0.0386\ W\Delta_g h'}{\delta_i \sqrt{\theta_i}} \tag{38}$$

Nozzle and rotor-blading losses. - Nozzle and rotor-blading aerodynamic losses are considered as the differential between ideal and gross power and are not directly determined herein.

Disk-windage loss. - The disk-windage loss is calculated according to equation (15), where

$$K_{II} = 1.272$$

$$\text{disk power loss} = 1.272 \left(\frac{\rho_d d_h u_h}{\mu_d}\right)^{-0.12} \left(\frac{N}{1000}\right)^3 d_h^5 \rho_d \frac{1}{\delta_i^{0.88} \theta_i^{0.632}} \tag{39}$$

The value of 1.272 for the empirical constant is dependent upon the type of disk shrouding and was obtained from the smaller turbine used. This value is considered to be applicable generally to configurations similar to that shown in figure 7. The density term used in the equation represents the average of the densities on both sides of the disk.

Bearing loss. - Bearing power loss is calculated from equation (16). The weight flow of oil was determined from the

1032

calibration of the lubricating system mock-up. The temperature rise of the oil was obtained from thermocouples in the oil lines before and after each bearing. The specific heat of the oil was based on the mean oil temperature in the bearing.

Pumping loss. - This partial-admission loss was calculated from equation (21), using an experimentally determined

$$\lambda = 15.19$$

and the equation then corrected to sea level to give

$$\text{pumping loss} = \frac{15.19 \left(\frac{l}{D}\right) D^5 \left(\frac{N}{1000}\right)^3 (1-F) \rho_d}{\delta_i \sqrt{\theta_i}} \qquad (40)$$

This equation, which has the advantage of dimensional correctness, may be adjusted for a particular application merely by selection of the term λ. In general,

λ = 27.99 for uncovered inactive blading

= 12.93 for inactive blading having a cover with a 3/16-inch clearance

The configuration investigated does not correspond to either of the preceding conditions for which a numerical value for λ is listed, but is somewhere between the two. In order to determine a more appropriate value for the constant, the smaller turbine, previously mentioned, which had a configuration substantially similar to that shown in figure 7, was motored and measurements of the pumping loss were obtained. The pumping-loss expression was rearranged to make λ the dependent variable, and values of λ were obtained over a wide range of rotor speeds and gas densities.

Little variation in the value of the coefficient was encountered and a mean value of 15.19 was obtained for λ.

Driving-fluid losses. - Because of the difficulties involved in obtaining gas-state measurements to evaluate driving-fluid losses, these losses were experimentally determined for this turbine and compared with the general expression, equation (27), to verify that the losses do vary as $K_{III} \bar{\rho}_i N$.

The driving-fluid losses are experimentally evaluated at 120° and 180° admission, using equation (26); the blade power was

calculated by use of equation (4). The driving-fluid losses for other degrees of admission are therefore established by equation (28), which becomes

$$(\text{driving-fluid loss})_F = \frac{3}{2}(1-F)\,(\text{driving-fluid loss})_{120^\circ} \quad (41)$$

This relation has been verified at 180° admission.

Presentation Methods

Performance presentation. - Turbine performance for full and partial admission is presented in the form of a "carpet" plot (fig. 8). The procedure is an adaption of the methods of presentation of experimental results outlined in reference 7. Absence of an abscissa in the figure is to be noted. This composite or carpet plot is obtained by first plotting the corrected power output as the ordinate against total-pressure ratio as the abscissa with rotor speed as a parameter. (See diagram (a).)

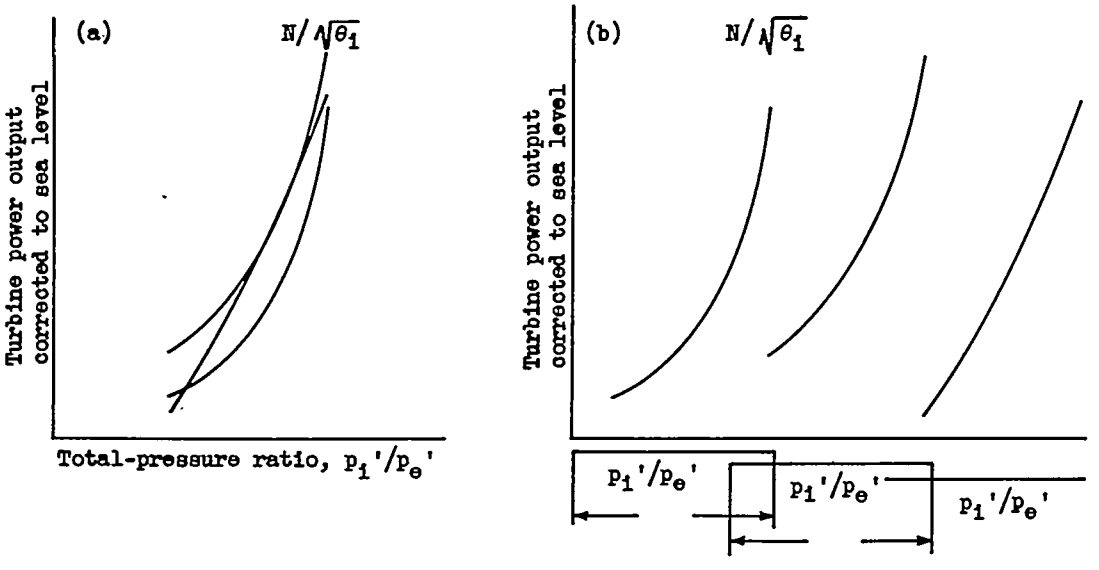

The curves (each representing constant speeds) may then be separated by displacing each curve, together with its abscissa, to the right a convenient distance X proportioned to the rotor speed. The result is a series of vertically oriented plots of corrected power output against pressure ratio with the curves of lower speed at the left and the speeds increasing towards the right. (See diagram (b).)

All these curves, each representing a constant corrected rotor speed, cover the same range of pressure ratios and so permit construction of horizontal curves connecting points of equal values of pressure ratio on the constant speed curves. (See diagram (c).)

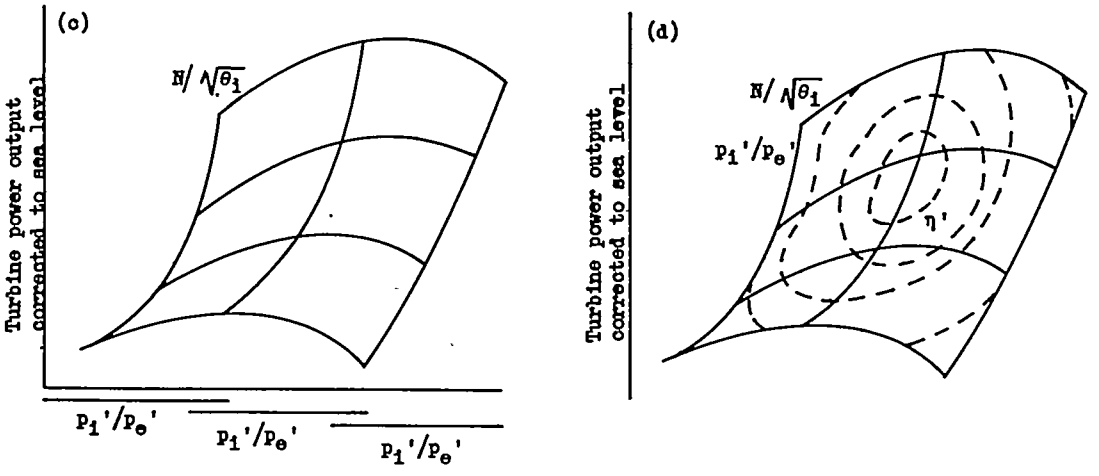

These curves of constant pressure ratio perform the same function as do the series of pressure-ratio abscissas associated with the constant-speed curves, so that the abscissas may be removed. In this manner a performance grid can be readily constructed upon which may be superimposed contours of constant over-all efficiency. (See diagram (d).)

The utility of this form of performance presentation becomes apparent if consideration is given to the information regarding

the operating characteristics of the turbine, which is either indicated directly or is obtained by readily performed calculations. As an illustration, the corrected power output, total-pressure ratio, corrected rotor speed, and over-all efficiency for a given inlet total pressure and temperature may be observed directly for two amounts of admission; whereas such quantities as weight flow, theoretical power input, discharge static pressure, ratio of inlet total pressure to discharge static pressure, theoretical blade-to-jet speed ratio, and turbine efficiency based on ratio of inlet total pressure to discharge static pressure may be computed. The method by which these quantities may be computed from a performance presentation like figure 8 follows.

(1) theoretical power input based on stagnation conditions

$$= \frac{\text{power output corrected to sea level}}{\text{efficiency based on total-pressure ratio}}$$

$$\frac{W(\Delta_s h')}{0.707} = \frac{P}{\eta'} \tag{42}$$

(2) weight flow

$$= \frac{\text{theoretical power input based on stagnation conditions}}{\text{ideal enthalpy drop per pound fluid based on stagnation conditions}}$$

$$W = \frac{\left[\frac{W(\Delta_s h')}{0.707}\right]}{\left[\frac{(\Delta_s h')}{0.707}\right]} \tag{43}$$

When the inlet total temperature and total-pressure ratio are known, the ideal power per pound of driving fluid may be obtained by use of tables in reference 8.

(3) discharge total pressure $= \frac{\text{inlet total pressure}}{\text{total-pressure ratio}}$

$$p_e' = \frac{p_i'}{\left(\frac{p_i'}{p_e'}\right)} \tag{44}$$

(4) discharge static pressure p_e, from the following equation

$$\frac{p_e'}{p_e} = \left[\frac{1}{2} + \sqrt{\frac{1}{4} + \frac{1}{2g}\frac{\gamma-1}{\gamma}\left(RT_1' - \frac{\gamma-1}{\gamma}\,550\,\frac{P}{W}\right)\left(\frac{W}{70.73\,p_e A_e}\right)^2}\right]^{\frac{\gamma}{\gamma-1}} \tag{45}$$

where

A_e discharge area, (sq ft)

It is to be noted that the power term in equation (45) should utilize blade power; however, shaft power, an easily measurable quantity, has been substituted with resulting error so slight as to be negligible.

(5) ratio of inlet total pressure to discharge static pressure

$$= \frac{\text{inlet total pressure}}{\text{discharge static pressure}}$$

$$= \frac{p_i'}{p_e} \tag{46}$$

(6) efficiency based on ratio of inlet total pressure to discharge static pressure

$$= \frac{\text{net power output}}{\text{ideal power input based on ratio of inlet total pressure to discharge static pressure}}$$

$$\eta = \frac{P}{\left[\frac{W(\Delta_s h)}{0.707}\right]} \tag{47}$$

When the inlet total temperature and ratio of inlet total pressure to discharge static pressure are known, the ideal power input per pound of driving fluid based on ratio of inlet total pressure to discharge static pressure may be obtained by use of tables in reference 8.

(7) blade pitch-line velocity u_m from the following equation

$$u_m = \pi D \left(\frac{N}{60}\right) \tag{48}$$

(8) theoretical jet velocity V_j' based on ratio of inlet stagnation pressure to discharge stagnation pressure, from the following equation

$$V_j' = \sqrt{2gJc_pT_i' \left[1 - \frac{1}{\left(\frac{p_i'}{p_e}\right)^{\frac{\gamma-1}{\gamma}}}\right]} \tag{49}$$

where J is the mechanical equivalent of heat.

(9) theoretical jet velocity V_j based on ratio of inlet total pressure to discharge static pressure, from the following equation

$$V_j = \sqrt{2gJc_pT_i' \left[1 - \frac{1}{\left(\frac{p_i'}{p_e}\right)^{\frac{\gamma-1}{\gamma}}}\right]} \tag{50}$$

(10) velocity ratio ν' based on ratio of inlet total pressure to discharge total pressure, from the following equation:

$$\nu' = \frac{u_m}{V_j'} \tag{51}$$

(11) velocity ratio ν based on inlet total pressure to discharge static pressure, from the following equation:

$$\nu = \frac{u_m}{V_j} \tag{52}$$

A numerical illustration of these calculations is presented in appendix B.

1032

Loss-presentation method. - The power losses corrected to sea level are plotted against corrected turbine rotor speed in figure 9 at a total-pressure ratio of 2.0 with the degree of admission as parameter where applicable. Disk-friction losses are so small that they are not shown in figure 9.

The ideal power, net power, and applicable losses per pound of driving fluid, all corrected to sea-level conditions, at a pressure ratio of 2.0, are plotted against corrected rotor speed for 360° (full), 180°, and 120° admissions in figure 10.

Performance-Estimation Method

The turbine power outputs at any two amounts of admission are related by the change in the loss quantities. It is therefore possible to obtain estimates of power output at any degree of admission by making use of the full-admission carpet plot and the loss curves. From equation (30) it can be seen that

$$(\text{net power estimated})_F = F\,(\text{power observed})_{360^\circ} + (\text{shaft losses})_{360^\circ} - (\text{shaft losses})_F - (\text{driving-fluid losses})_F \qquad (53)$$

In order to estimate power at any degree of admission, it remains to evaluate these losses at some degree of admission and to know the manner of variation of the losses with admission. As previously described, disk-friction and bearing losses are invariant with admission, and pumping loss and driving-fluid losses are proportional to the inactive nozzle arc.

When the power output has been estimated at any degree of admission with equation (53) the efficiency for that degree of admission can be easily estimated from equation (33). A numerical example is provided in appendix B.

This simplified method quickly yields good approximations. Upon correction of the turbine output and of correctable losses to sea level, the bearing loss, which has no correction applied, forms a disproportionately large part of the corrected power. This disproportion in turn affects the accuracy of the efficiency estimations based

on the use of corrected data. Some additional accuracy is therefore gained by use of operational data uncorrected to sea level in equation (53).

This modified procedure has been followed in the construction of figure 11 in which is plotted over-all turbine efficiency against percentage of full-power output with degree of admission as parameter. Included in the range of turbine operation at full admission is the point close to the design operating condition, which is a corrected rotor speed of 8650 rpm, a total-pressure ratio of 2.08, and an inlet total pressure of 45 inches of mercury absolute at the test operating temperature of 800° R (based on constant design Reynolds number index $p_1'/(T_1')^{1.1}$, reference 6). In order to obtain an indication of the turbine performance at other values of admission, the conditions of operation were arbitrarily selected to be maintained constant at this equivalent design point while estimates of performance were made at several reduced admissions. Because the maximum corrected power output in these experiments occurs at a pressure ratio of 2.4 rather than 2.0, the power at the equivalent design point for full admission represents approximately 83 percent of this value.

Comparison of Partial Admission with Other Methods of Power Reduction

Turbine-inlet pressure, pressure ratio, and active nozzle arc are evaluated as power-control parameters in figure 12. Turbine over-all efficiency is plotted against the percentage of full-power output for a constant inlet total temperature of 800° R and a corrected rotor speed of 8650 rpm. Lines of constant inlet total pressure and total-pressure ratio enclose areas at both full and 120° admission within which turbine performance was investigated. In order to isolate the turbine performance from any interaction with a compressor, the driving fluid was assumed to be delivered to the turbine from an external source at a constant pressure of 45 inches of mercury absolute. Reduction of the inlet pressure to lower values is accomplished by throttling, the accompanying loss being charged to the turbine. This procedure accounts for the largest part of the severe loss in efficiency at the lower pressures. The projected distance of these areas on the abscissa gives an indication of the flexibility of power control.

Superimposed on the plot is the curve representing power regulation by means of active nozzle-arc control at a constant pressure ratio of 2.0, which is shown in figure 11. The partial-admission

control curve in figure 12 serves an additional purpose in that it orients the areas of turbine operation at any degree of admission with respect to corresponding areas at other degrees of admission. This orientation permits rapid visual estimates to be made regarding the characteristics for all mutual relations of these control parameters.

In figure 13, the parameter of corrected rotor speed is introduced. The construction of the plot is similar to that of figure 12 with the exception that corrected rotor speed replaces inlet pressure as a variable. For the plot shown in figure 13, the inlet total pressure is maintained constant at 45 inches of mercury absolute.

Because the points of peak efficiency occur at lower speeds with decreasing pressure ratio, the planes formed by the operational areas appear to fold back upon themselves, with the effect magnified at the lower admissions.

ACCURACY

The calculated probable error in the over-all efficiency over most of the range of turbine operation is within ±1 point. Power-output calculations over this range are accurate within ±1/2 percent of the true net power output. The greatest error occurs at the lowest power levels with reduced admission, reduced inlet pressure, and high rotor speed. At these conditions, efficiency is accurate within ±2 points and power output is accurate within ±4.6 percent.

Temperature readings are considered accurate to ±5° R, turbine speed measurements to ±5 rpm, turbine-torque estimates to ±15.09 inch-pounds, and manometer readings to ±0.05 inch of mercury.

The accuracy of the power estimates based on the more refined methods, using uncorrected data, as were used in the construction of figure 11, is within ±1 percent of the observed data over most of the speed range and within ±3 percent at the highest speeds. Turbine-over-all-efficiency estimates by this method are within ±1 point over most of the speed range and within ±1½ points at the lower and higher ends of the speed range.

Estimates of power output for 180° admission by the method based on use of corrected data are approximately 1 percent lower than the estimations that use the more refined method based on observed data. The efficiency estimated for 180° by this rapid method is approximately 1 point lower than the estimation obtained

from data uncorrected to sea level. Efficiency estimations performed this way will always be lower than those shown in figure 11, becoming 3 points lower at 90° admission.

RESULTS

Losses

With the exception of disk-windage loss, a quantitative statement of the types of turbine loss that have been considered is presented in figure 9. These quantities are based on data obtained at an inlet pressure of 45 inches of mercury absolute and a total-pressure ratio of 2.0. Because the losses are expressed in corrected form, they may be considered representative of the losses at other inlet pressures, although all the losses except bearing losses would require adjustment for changes in pressure ratio.

Presented in figure 9 are the losses as functions of corrected rotor speed for a range of admissions from 90° to 360°, where applicable. Use of logarithmic scales for abscissas and ordinates results in the slopes of these loss curves being equal to the exponential rate of rotor speed at which the losses vary.

Rotor-tip leakage loss. - Estimates of rotor-tip leakage losses for a range of gas admissions are plotted in figure 9(a). Because the tip leakage is invariant with rotor speed, the curves appear as horizontal lines over the range of corrected rotor speeds.

Disk-windage loss. - In general, disk-windage loss forms a small fraction of the dissipated power output, which is exemplified by the results of these studies where the maximum value of the corrected disk loss amounted to less than 1 horsepower at the highest corrected operating speed of 14,000 rpm. Because of the minor nature of this loss, it does not appear in figure 9. However, were the disk vaned, as is the case for some commercial gas turbines, the additional pumping action would act to increase greatly the disk power loss.

Bearing loss. - Bearing loss is plotted against corrected rotor speed in figure 9(b). The single bearing-loss curve is considered applicable for any degree of admission. The temperature rise of the oil across the journal-thrust bearing did not decrease for the runs with partial admission indicating little change in the thrust-bearing losses. At the higher speeds, the bearing-loss curve approaches a 1.4-power variation with the speed. That this loss is

not a second-power variation, as would be expected, is attributed to inaccuracy of the experimental method employed. The error involved, however, is slight, if not negligible.

Pumping loss. - Pumping losses are shown in figure 9(c) for the range of admissions considered. The curves serve to demonstrate the increase of this partial-admissions loss with increased blocking. As is indicated by equation (21), this loss varies as the third power of the rotor speed.

The importance of this loss in a particular application is determined largely by the pitch-line diameter of the turbine because the pumping loss varies as the fourth power of the pitch-line diameter.

Driving-fluid losses. - The driving-fluid losses are presented in figure 9(d) for several degrees of admission. Because these losses are directly proportional to rotor speed, the curves appear as straight lines with a slope of unity. For this turbine, it is noted that the driving-fluid losses are quite large as compared with the other losses considered.

Analysis of the turbine data confirms that the driving-fluid losses due to partial admission as expressed by equation (27) are representative of actual performance. The power difference representing the driving-fluid losses is experimentally found to be proportional to the reduction of active nozzle arc and may be correlated by the product $K_{III}\rho_1 N$ over most of the operating range. Verification of this analysis is provided in figure 14, where the driving-fluid losses for 180° and 120° admission are experimentally determined. From full-admission data by use of equation (19), the gross powers at 180° and 120° admission are obtained. The blade power for each of these partial admissions is found, as in equation (4), from the observed net power output plus the shaft losses obtained from figures 9(b) and 9(c). These power terms are then plotted against corrected rotor speed and, according to equation (26), (blade power at full admission being equal to gross power at full admission) the driving-fluid losses, identified by the shaded areas, are obtained as the difference between the gross powers and the blade powers for each of these two admissions, respectively.

It can be seen from figure 14 that the driving-fluid losses are proportional to the rotor speed and likewise proportional to the amount of nozzle blocking. Driving-fluid losses may therefore be properly expressed by equation (27) and related at various degrees of admission by equation (28).

By dimensional analysis, it can be seen that only the driving-fluid losses vary as $K_{III}\bar{\rho}_i N$ and therefore shaft or tip leakage losses cannot be made to correlate the power differentials observed. This fact rules out the possibility that the power differences can be accounted for by errors in the magnitudes of the shaft losses as calculated by the empirical equations presented.

Nozzle and rotor-blading losses. - The nozzle and rotor-blading aerodynamic losses are presented for the range of admissions in figure 9(e). These losses may be seen in the figure to be directly proportional to the degree of admission. By comparison with figures 8(a) and 8(b), it can be seen that the nozzle and rotor-blading aerodynamic losses are minimal at the speed range corresponding to the peak operating efficiencies of the turbine.

Loss relations. - Represented in figure 10 is a quantitative analysis of the manner in which the ideal power per pound (specific ideal power) is dissipated by the various losses at 360° (full), 180°, and 120° admissions. All the quantities are corrected to sea-level conditions. Because the ideal power per pound of driving fluid is independent of the degree of admission, comparison of the magnitudes of these losses at the various degrees of admission enables a direct evaluation of the relative effect of each of the losses on the net power output with reduction of the active nozzle arc.

From figure 10 it can be seen that the specific rotor-tip leakage loss is constant for all degrees of admission and for all rotor speeds.

The bearing power loss of the turbine is independent of the percentage of active nozzle arc; therefore the specific bearing loss is inversely proportional to the weight flow and hence to the degree of admission. As indicated earlier, the bearing losses are proportional approximately to the 1.4 power of the rotor speed.

At any given degree of admission, the pumping losses are proportional to the cube of the rotor speed, whereas the driving-fluid losses are directly proportional to rotor speed.

The pumping and driving-fluid losses were shown, in the ANALYSIS section, to be proportional to the inactive nozzle arc and in figure 10 may be seen to vary in this manner.

The nozzle and rotor aerodynamic losses per pound of driving fluid are independent of the degree of admission and consequently are the same for the three admissions presented in figure 10.

Disk loss cannot be presented clearly in figure 10 because it is too small.

1032

The corrected specific net power, which is ideal power minus all the losses, is shown in figure 10 for each of the three turbine configurations. The specific net power when multiplied by the weight flow is in agreement with the corrected turbine output for full and 120° admission shown in figure 8(b).

Full-Admission Performance

The turbine operating characteristics for full-admission operation are presented as a composite plot, constructed as previously outlined in the section entitled METHODS. The turbine design operating conditions are indicated in figure 8(a) as point D, which falls well within the turbine operating range covered in this investigation. The turbine design operating point D is seen to be within 1/2 point of the maximum efficiency observed. The island formed by the peak operating efficiency contour of 76 percent is centered at a corrected rotor speed of 9500 rpm at a total-pressure ratio of 2.2. The power output at this point is 412 horsepower corrected to sea level, which corresponds to approximately 3250 horsepower at full-scale operation.

Operation outside of this island is accompanied by decreasing efficiencies. However, when changes in pressure ratio are accompanied by adjustments in rotor speed to maintain the most favorable blade-to-jet speed ratio, the gradient of efficiency is minimized to a drop of 3 points over the entire pressure-ratio range.

The range of turbine power output is represented in figure 8(a) as vertical distances, which are seen to increase to the right on this plot. This increase is due to the effects of pressure-ratio changes being most pronounced at higher rotor speeds.

Partial-Admission Performance

The performance characteristics of this turbine at 120° admission over the same range of operating conditions as at full admission are presented in the form of a carpet plot in figure 8(b). This carpet is superimposed on the one previously presented in figure 8(a) for full admission to enable ready comparison of operation with full and partial admission.

Of primary significance are the reductions in over-all turbine efficiency encountered with reduced admission. The data indicate that a drop of 16 points in the peak efficiency is obtained when the active nozzle arc is decreased to 120°. The drop is caused by the special losses that are introduced when only a fraction of the nozzle arc is active. When the turbine power output is controlled by nozzle cut-out, the velocity diagrams for equivalent operating conditions at reduced admissions remain largely unchanged, an advantageous feature in power regulation by means of active-nozzle-arc control. This effect is demonstrated in figure 8(b), where the performance patterns over the range of rotor speed and pressure ratio are similar for full and 120° admissions. Because the over-all efficiency is based on the turbine net power output, increases in the power extraction caused by the additional partial-admission losses are evidenced by a change in the position of the efficiency contours. Rapid increases of the driving-fluid and pumping losses with rotor speed cause the region of peak performance to be shifted toward lower rotor speeds with increasing nozzle cut-out, and the adjustments in rotor speed required to maintain optimum blade-to-jet speed ratios with changes in rotor speed remain virtually unchanged. In the upper speed region, the change in net turbine power per pound of driving fluid in response to a given change in pressure ratio is diminished with reduction of the active nozzle arc. The reduced net power range is attributed to the more pronounced effects of the partial-admission losses with increasing rotor speeds.

1032

Partial Admission as a Means of Power Control

The application of partial admission as a means of power control is evaluated in figure 11 in the form of a curve of over-all turbine efficiency plotted against the percentage of full-power output. At full, 180°, and 120° admission, the values expressed are based on experimental data, the remainder of the curve was constructed using the performance-prediction technique previously described. The curve indicates that, for a constant turbine operating condition, partial admission represents an effective means of power control up to 180° of nozzle-arc reduction. Power control by cut-out of more than one-half of the nozzles is accompanied by a prohibitive drop in over-all efficiency due to the increasingly severe effect of the turbine losses. For other turbine operating conditions, the general shape of this curve is similar except that the performance falls off more sharply with the intensifying effect of the partial-admission losses at higher speeds. This effect, however, is not too important because a primary feature of partial-admission power control is that the turbine operating conditions

are maintained at the design point and there would be little requirement for operation in the more unfavorable regions.

Comparison of Partial Admission with Other Power-Control Methods

Turbine-inlet pressure and total-pressure ratio are evaluated as power-control parameters in figure 12. For a given admission, there appear to be about equal ranges of power control using either inlet pressure or pressure ratio as the controlling parameter. However, with respect to over-all efficiency, the curves indicate that no advantage is gained by inlet-pressure control either exclusively or in combination with pressure-ratio control. The same power reduction can be accomplished through use of pressure-ratio control independently of inlet-pressure control and at considerably higher efficiencies. Comparison of the methods shows that partial admission offers a more flexible system while maintaining a corresponding trend with regard to efficiency.

Turbine-rotor speed appears as a power-control parameter in figure 13. As is evidenced in the figure, power control by means of pressure ratio offers a more flexible system than that utilizing rotor speed. Some benefit may be realized, however, particularly at lower admissions, if the rotor speed is manipulated over a range sufficient to take advantage of the gains in efficiency available at the lower pressure ratios. That the power-control curves terminate with a total-pressure ratio of 1.5 should not be taken to mean that further power reduction is not obtainable by even lower pressure ratios. In these studies, the turbine was not operated below this value and no data are available. Judging from the trends in evidence at the lowest pressure ratio shown, further power reduction by diminishing pressure ratio must be accompanied by increasingly severe speed regulation if the optimum turbine efficiencies are to obtain. Reductions in both speed and pressure ratio are attended by increased turbine-discharge temperatures, which impose, as a further limitation to this system of power control, the highest turbine-discharge temperature that may be sustained for any length of operation. The partial-admission control curve, which is superimposed on figure 13, again serves to orient the operational areas at various degrees of active nozzle arc.

Because all data were obtained in this investigation at a constant inlet temperature, little can be said concerning the effects of variable inlet temperature as a control parameter. A brief analysis would show that such a system is very restricted as regards flexibility of power output, but the small reductions permitted (on the order of 10 to 20 percent of full power) are obtained with a negligible reduction in the efficiency.

DISCUSSION

Because reductions in efficiency with partial-admission operation may be ascribed in large part to the induced losses, it is worthwhile examining these losses briefly with the idea of devising means to reduce or eliminate them. As has been mentioned previously, there are two principal types of loss that occur with partial admission: pumping losses and driving-fluid losses. In reference 4 (pp. 199-200), it is shown that pumping losses may be effectively reduced by closely shrouding the inactive rotor blading. Such shrouding would also serve to reduce that part of the driving-fluid loss caused by induced gas diffusion at the nozzle discharge as follows: (1) It would decrease the pressure gradient between the active and inactive flow regions of the blading, and (2) it would eliminate the flow of the diffused gases through the inactive rotor blading and the subsequent power loss. The method proposed in reference 4 (p. 221) is aimed at reducing the scavenge and eddy losses by more careful control of the flow to the rotor at the start and end of the active cycle.

These and other refinements, although not employed in this investigation, are worth consideration in the design of a partial-admission power plant.

A turbine operating with partial admission is subject to induced rotor-blade vibrations in addition to those encountered with full-admission operation. During normal turbine operation, when the period of the intermittent force applications from the individual nozzles is the same as a natural vibration period of the blades, secondary resonance (reference 9) occurs. This secondary resonance is characteristic of turbines both at full admission and during the active cycle at partial admissions. Harmful stresses resulting from secondary resonance may be averted by proportioning the blades to secure a suitable mass-stiffness ratio and provide sufficient internal damping to maintain the vibration amplitudes at a safe low level.

Primary resonance, as defined in reference 9, occurs at partial admission when the forced vibration set up by the application and release of the driving-fluid force at the beginning and the end of cut-off (fig. 5) has the same period as a natural vibration frequency. One or more operating conditions will always exist during partial-admission operation at which the timing of the loading and the unloading of the blades in the manner described will be such as to cause primary resonance. Precautions must therefore be taken in the design of the rotor blading so that, under conditions of primary resonance, the maximum blade stresses induced may be withstood safely.

A method proposed in reference 4 (p. 221) would serve to reduce the rate of blade loading and unloading, which would act to alleviate the blade-vibration problem.

No special precautions were taken against critical induced resonance for this investigation and no vibration difficulties were encountered in the turbine used. This fact is attributed to the reduced blade loading at low pressures and temperatures of the gas, so that, whereas conditions of primary and secondary resonance may have been present, the reduced blade loading resulted in relatively small blade stresses that could be safely withstood. There is no assurance that this would have been the case at full-load operation.

RESULTS AND CONCLUSIONS

From an investigation of the performance of a gas turbine over a range of operating conditions for full and partial admissions, the following results were obtained and conclusions drawn:

1. The efficiency and specific power output of a gas turbine operating with partial admission are primarily determined by the quantity of the special losses that are induced as the fraction of active nozzle arc is decreased.

2. Estimations of the over-all turbine efficiency and power output at any degree of admission were made possible by procedures correlating full- and partial-admission performance, which were developed on the basis of studies of these losses.

3. The efficiency estimations were within ±1 point of observed values over most of the speed range and within $\pm 1\frac{1}{2}$ points at the lower and higher ends of the speed range. The power estimates were within ±1 percent of observed data over most of the speed range and within ±3 percent at the highest speeds.

4. When no special precautions are taken to avoid losses, operation of a gas turbine with more than half of the nozzles inactive is accompanied by large reductions in the over-all efficiency.

5. Turbine power reduction by means of nozzle cut-out offers a high degree of flexibility while maintaining efficiencies comparable to those of the other methods of power control considered.

6. Considerable utility of the performance data is afforded by use of the convenient method presented for plotting the turbine characteristics. The method further serves to condense large quantities of data into a single composite plot.

7. In addition to secondary rotor-blade vibration encountered in any operating gas turbine, provisions are required to avoid or withstand the effects of primary rotor-blade vibrations induced by partial-admission operation.

Lewis Flight Propulsion Laboratory,
National Advisory Committee for Aeronautics,
Cleveland, Ohio, October 5, 1948.

APPENDIX A

SYMBOLS

The following symbols are used in this report:

A	area, sq ft
a	velocity of sound at observed conditions, ft/sec
B	number of active rotor blades at any instant
b	total number of blades in turbine rotor
C	blade radial tip clearance, ft
c	absolute velocity, ft/sec
c_p	specific heat at constant pressure, Btu/(lb)(^oF)
D	pitch-line diameter, ft
d	rotor-disk diameter, ft
F	fraction of active nozzle arc
G	fraction of active nozzle arc other than F
g	acceleration due to gravity, 32.174, ft/sec^2
$\Delta h'$	enthalpy drop based on ratio of inlet stagnation condition to discharge stagnation conditions, Btu/lb
$\Delta_s h$	isentropic enthalpy drop based on ratio of inlet stagnation conditions to discharge static conditions, Btu/lb
$\Delta_s h'$	isentropic enthalpy drop based on ratio of inlet stagnation conditions to discharge stagnation conditions, Btu/lb
J	mechanical equivalent of heat, 778, ft-lb/Btu
K_I	percentage of active gas through rotor-tip clearance space, constant for any particular turbine
K_{II}	empirical constant for disk-windage loss
K_{III}	empirical constant for driving-fluid losses

l	rotor-blade length, ft
M	Mach number
N	rotational speed, rpm
n	thickness coefficient (unity for reaction turbines)
P	turbine-shaft power output, corrected to sea-level conditions, hp
p	absolute pressure, lb/sq ft or in. Hg
R	gas constant, 53.345, ft-lb/(lb)($^{\circ}$F)
Re	Reynolds number
r	radius, ft
T	temperature, $^{\circ}$R
ΔT_{oil}	temperature rise of lubricating oil in bearings
u	velocity, ft/sec
V	gas velocity, ft/sec
V_j	theoretical jet velocity based on ratio of inlet total pressure to discharge static pressure, ft/sec
V_j'	theoretical jet velocity based on ratio of inlet total pressure to discharge total pressure, ft/sec
W	weight flow, lb/sec
z	total number of blades in turbine rotor
β_2	rotor-blade exit angle relative to plane of rotor disk measured at pitch line, deg
γ	ratio of specific heats of gas
δ	pressure correction ratio, p/p_0
η	turbine over-all efficiency based on ratio of inlet stagnation conditions to discharge static conditions

η'	turbine over-all efficiency based on ratio of inlet stagnation conditions to discharge stagnation conditions
θ	temperature correction ratio, T/T_0
λ	empirical constant, depending upon inactive blade shrouding
μ	absolute viscosity, (lb)(sec)/sq ft
ν	velocity ratio based on ratio of inlet total pressure to discharge static pressure
ν'	velocity ratio based on ratio of inlet total pressure to discharge total pressure
ρ	mass density, slugs/cu ft

Subscripts:

d	fluid surrounding turbine-rotor disk
e	turbine discharge (measuring station)
F	degree of admission corresponding to fraction of active nozzle arc
G	degree of admission corresponding to fraction of active nozzle arc other than F
h	hub or inner radius position (blade root)
i	inlet (measuring station)
j	jet
m	pitch line
s	isentropic
T	tip or outer-radius position
u	tangential
x	axial
0	NACA sea-level air

1	rotor inlet
2	rotor discharge
360°	full admission
120°	120° admission
180°	180° admission

Superscripts:

– (bar)	average value
' (prime)	stagnation state

APPENDIX B

CALCULATIONS

Numerical examples illustrating the calculation methods described in the text are presented.

Calculations from Figure 8

The operating characteristics of this turbine are computed from the information presented in figure 8 at the design operating point D. For 360° admission, a rotor speed of 8650 rpm, and a total-pressure ratio of 2.1, power output corrected to sea level P equals 388 horsepower; efficiency based on total-pressure ratio η' is 0.755; inlet total or stagnation temperature T_i' is 518.6° R; and inlet total or stagnation pressure p_i' equals 29.92 inches of mercury absolute.

The following quantities may be calculated:

1. Theoretical power input based on stagnation conditions from equation (42)

$$\frac{W(\Delta_s h')}{0.707} = \frac{P}{\eta'}$$

$$= \frac{388}{0.755}$$

$$= 514 \text{ hp}$$

2. Weight flow by equation (43)

$$W = \frac{\left[\frac{W(\Delta_s h')}{0.707}\right]}{\left[\frac{\Delta_s h'}{0.707}\right]}$$

From tables in reference 8,

$$\Delta_s h' = 23.76 \text{ Btu/lb}$$

therefore

$$W = \frac{514}{\left(\frac{23.76}{0.707}\right)}$$

$$= 15.29 \text{ lb/sec}$$

3. Discharge total pressure by equation (44)

$$p_e' = \frac{p_i'}{\left(\frac{p_i'}{p_e'}\right)}$$

$$= \frac{29.92}{2.1}$$

$$= 14.25 \text{ in. Hg absolute}$$

4. Discharge static pressure from equation (45)

$$\frac{p_e'}{p_e} = \left[\frac{1}{2} + \sqrt{\frac{1}{4} + \frac{1}{2g}\frac{\gamma-1}{\gamma}\left(RT_i' - \frac{\gamma-1}{\gamma}\cdot 550\,\frac{P}{W}\right)\left(\frac{W}{70.73\,p_e\,A_e}\right)^2}\right]^{\frac{\gamma}{\gamma-1}}$$

where

p_e' 14.25 in. Hg absolute

g 32.174 ft/sec^2

γ 1.4

R 53.345 ft-lb/lb/$^\circ$F

T_i' 518.6° R

P 388 hp

W 15.29 lb/sec

A_e 0.686 sq ft

Therefore

$$p_e = 10.80 \text{ in. Hg absolute}$$

5. Ratio of inlet total pressure to discharge static pressure by equation (46)

$$\frac{p_1'}{p_e} = \frac{29.92}{10.80}$$

$$= 2.770$$

6. Efficiency based on ratio of inlet total pressure to discharge static pressure by equation (47)

$$\eta = \frac{P}{\left(\frac{W\Delta_s h}{0.707}\right)}$$

From tables in reference 8,

$$\Delta_s h = 32.01 \text{ Btu/lb}$$

Therefore

$$\eta = \frac{388}{\left[\frac{(15.29)\ (32.01)}{0.707}\right]}$$

$$= 0.560$$

7. Blade pitch-line velocity u_m from equation (48)

$$u_m = \pi D \left(\frac{N}{60}\right)$$

where

D 1.167 ft

N 8650 rpm

Therefore

$$u_m = 528 \text{ ft/sec}$$

8. Theoretical jet velocity V_j' based on ratio of inlet to discharge stagnation pressures from equation (49)

$$V_j' = \sqrt{2gJc_p T_i' \left[1 - \frac{1}{\left(\frac{p_i'}{p_e'}\right)^{\frac{\gamma-1}{\gamma}}}\right]}$$

where

J 778 ft-lb/Btu

c_p 0.240 Btu/(lb)($^\circ$F)

therefore

$$V_j' = 1092 \text{ ft/sec}$$

9. Theoretical jet velocity V_j based on ratio of inlet total pressure to discharge static pressure by equation (50)

$$V_j = \sqrt{2gJc_p T_i' \left[1 - \frac{1}{\left(\frac{p_i'}{p_e}\right)^{\frac{\gamma-1}{\gamma}}}\right]}$$

Therefore

$$V_j = 1255 \text{ ft/sec}$$

10. Velocity ratio ν' based on ratio of inlet total pressure to discharge total pressure by equation (51)

$$\nu' = \frac{u_m}{V_j'}$$

$$= \frac{528}{1092}$$

$$= 0.4835$$

11. Velocity ratio ν based on ratio of inlet total pressure to discharge static pressure by equation (52)

$$\nu = \frac{u_m}{V_j}$$

$$= \frac{528}{1255}$$

$$= 0.421$$

Estimation of Power at 180° Admission

At 180° admission, equation (30) or (53) becomes

$$(\text{net power estimated})_{180^\circ} = \frac{1}{2}\left[(\text{power observed})_{360^\circ} + (\text{shaft losses})_{360^\circ}\right]$$

$$- (\text{shaft losses})_{180^\circ}$$

$$- (\text{driving-fluid losses})_{180^\circ}$$

At 180° admission, a corrected rotor speed of 8650 rpm, and a total-pressure ratio of 2.0,

$$(\text{power observed})_{360^\circ} = 365 \text{ hp, from figure 8}$$

$$(\text{pumping loss})_{360^\circ} = 0, \text{ from figure 9(c)}$$

$$(\text{bearing loss})_{360^\circ} = 6.9 \text{ hp, from figure 9(b)}$$

$$(\text{pumping loss})_{180^\circ} = 1.5 \text{ hp, from figure 9(c)}$$

$$(\text{driving-fluid loss})_{180^\circ} = 19.8 \text{ hp, from figure 9(d)}$$

Therefore

$$(\text{estimated power})_{180^\circ} = \frac{1}{2}(365 + 6.9) - (6.9 + 1.5) - 19.8$$

$$= 157.8 \text{ hp}$$

Because all quantities used were corrected to standard sea-level conditions, the estimated power for 180° is at standard sea-level conditions.

Estimation of Efficiency at 180° Admission

The over-all efficiency that may be expected at a given degree of admission may be calculated from equation (33) once the power for the same operating conditions has been estimated for that degree of admission.

At 180° admission, equation (33) becomes

$$\eta'_{180^\circ} = \frac{1}{\frac{1}{2}}\left(\frac{P_{180^\circ}}{P_{360^\circ}}\right)\eta'_{360^\circ}$$

$$P_{180^\circ} = 157.8 \text{ hp}$$

$$P_{360^\circ} = 365 \text{ hp from figure 8}$$

$$\eta'_{360^\circ} = 0.755 \text{ from figure 8}$$

$$\eta'_{180^\circ} = \frac{1}{\frac{1}{2}}\left(\frac{157.8}{365}\right) 0.755$$

$$= 0.653 \text{ estimated efficiency}$$

By comparison with figure 11, it may be seen that the estimated efficiency 0.653 is in close agreement with the value actually obtained by test for 180° admission.

REFERENCES

1. Kent, Robert Thurston: Mechanism and Mechanics. Kent's Mechanical Engineers' Handbook, sec. 8. John Wiley & Sons, Inc., 11th ed., 1938, p. 21.

2. Goudie, William G.: Steam Turbines. Longmans, Green and Co. (London), 2d ed., 1922, p. 535.

3. Culver, E. P.: Investigation of a Simple Form of Hydraulic Dynamometer. Mech. Eng., vol. 59, no. 10, Oct. 1937, pp. 749-753.

4. Stodola, A.: Steam and Gas Turbines. Vol. I. McGraw-Hill Book Co., Inc., 1927, pp. 199-200, 201, 221. (Reprinted, Peter Smith (New York), 1945.)

5. Moore, Charles S., Biermann, Arnold E., and Voss, Fred: The NACA Balanced-Diaphragm Dynamometer-Torque Indicator. NACA RB No. 4C28, 1944.

6. Gabriel, David S., Carman, L. Robert, and Trautwein, Elmer E.: The Effect of Inlet Pressure and Temperature on the Efficiency of a Single-Stage Impulse Turbine Having an 11.0-Inch Pitch-Line Diameter Wheel. NACA ACR No. E5E19, 1945.

7. Yates, A. H.: 'Carpets' and 'Lattices'. Aircraft Eng., vol. XVIII, no. 203, Jan. 1946, pp. 8-9.

8. Keenan, Joseph H., and Kaye, Joseph: Thermodynamic Properties of Air. John Wiley & Sons, Inc., 1945.

9. Allen R. C.: Steam-Turbine Blading. Trans. A.S.M.E., vol. 62, no. 8, Nov. 1940, pp. 689-705; discussion, pp. 705-710.

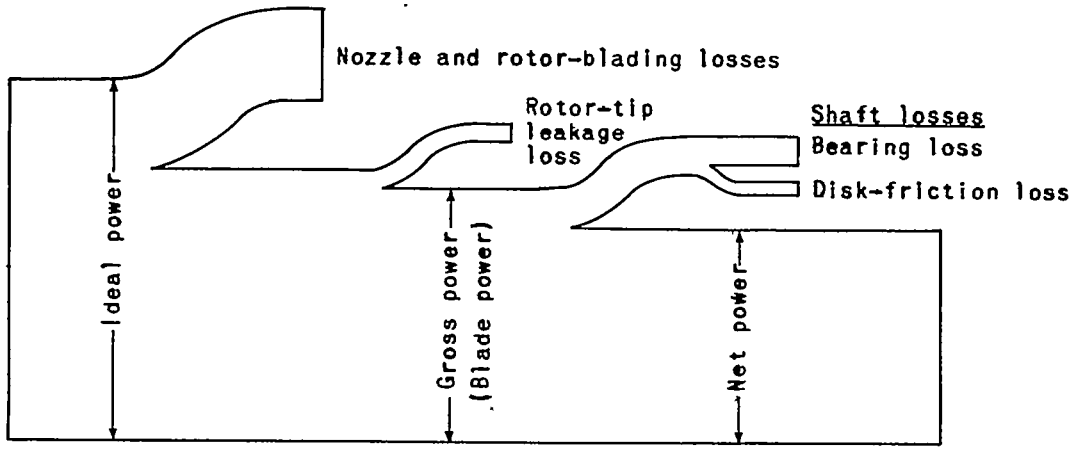

(a) Full admission (360°).

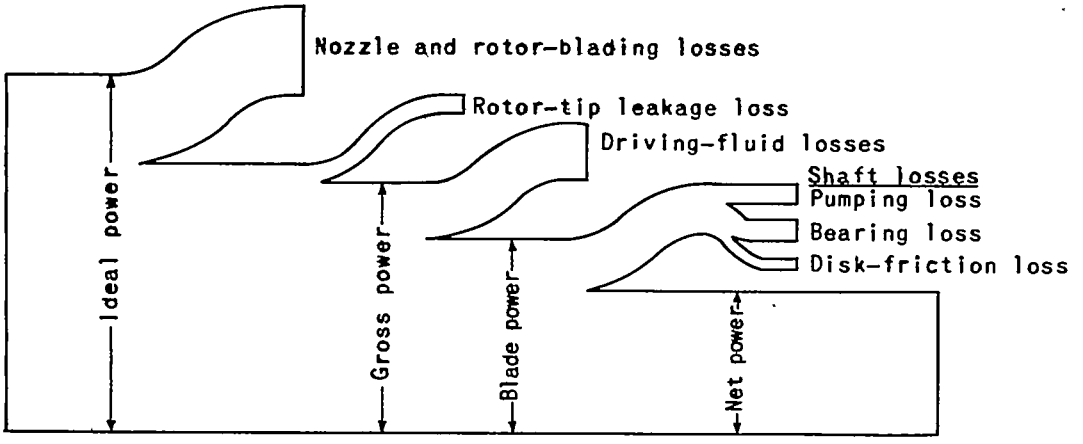

(b) Partial admission.

NACA

Figure 1. - Schematic relation of specific turbine-power concepts showing specific power-loss dissipations.

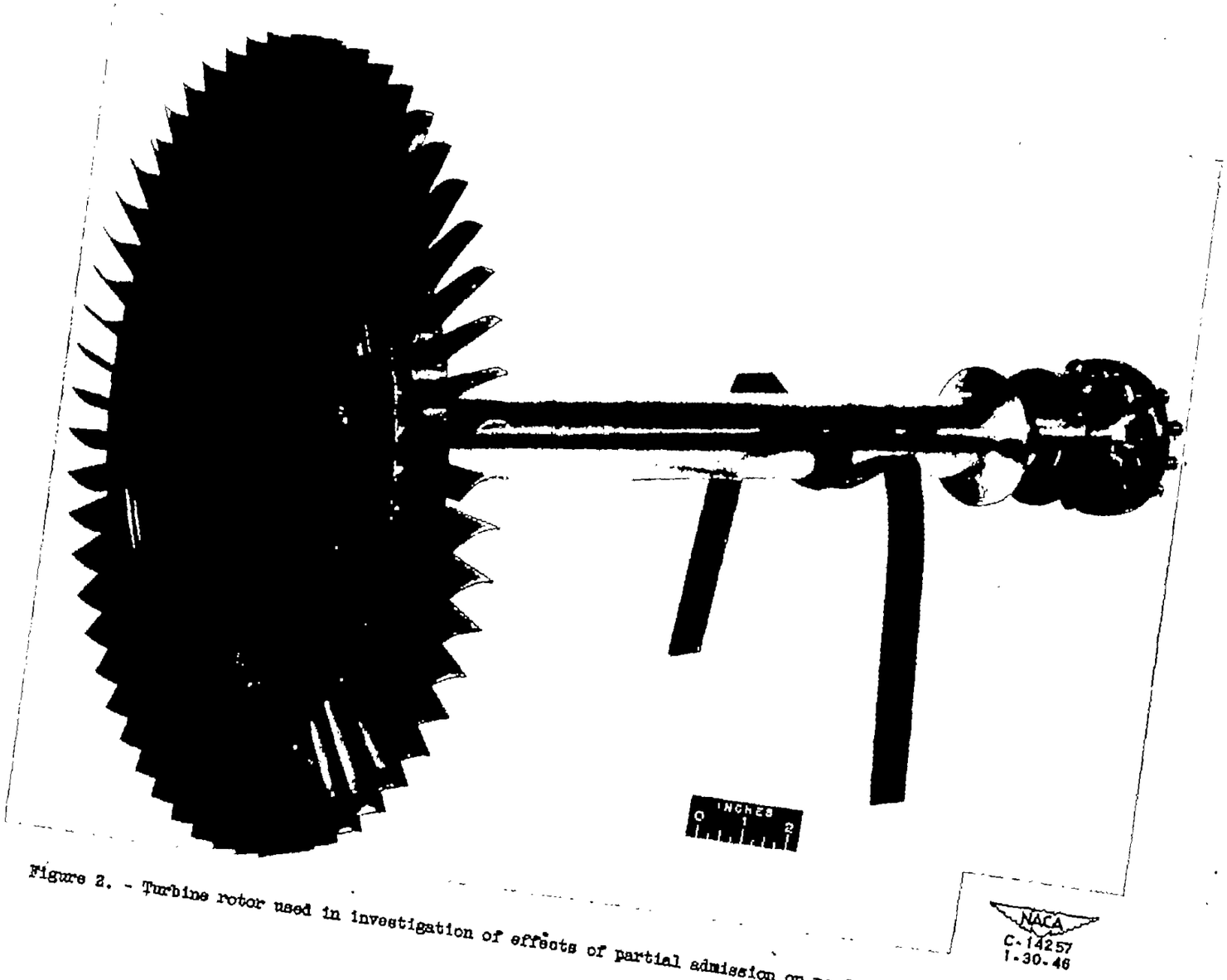

Figure 2. - Turbine rotor used in investigation of effects of partial admission on performance of gas turbine.

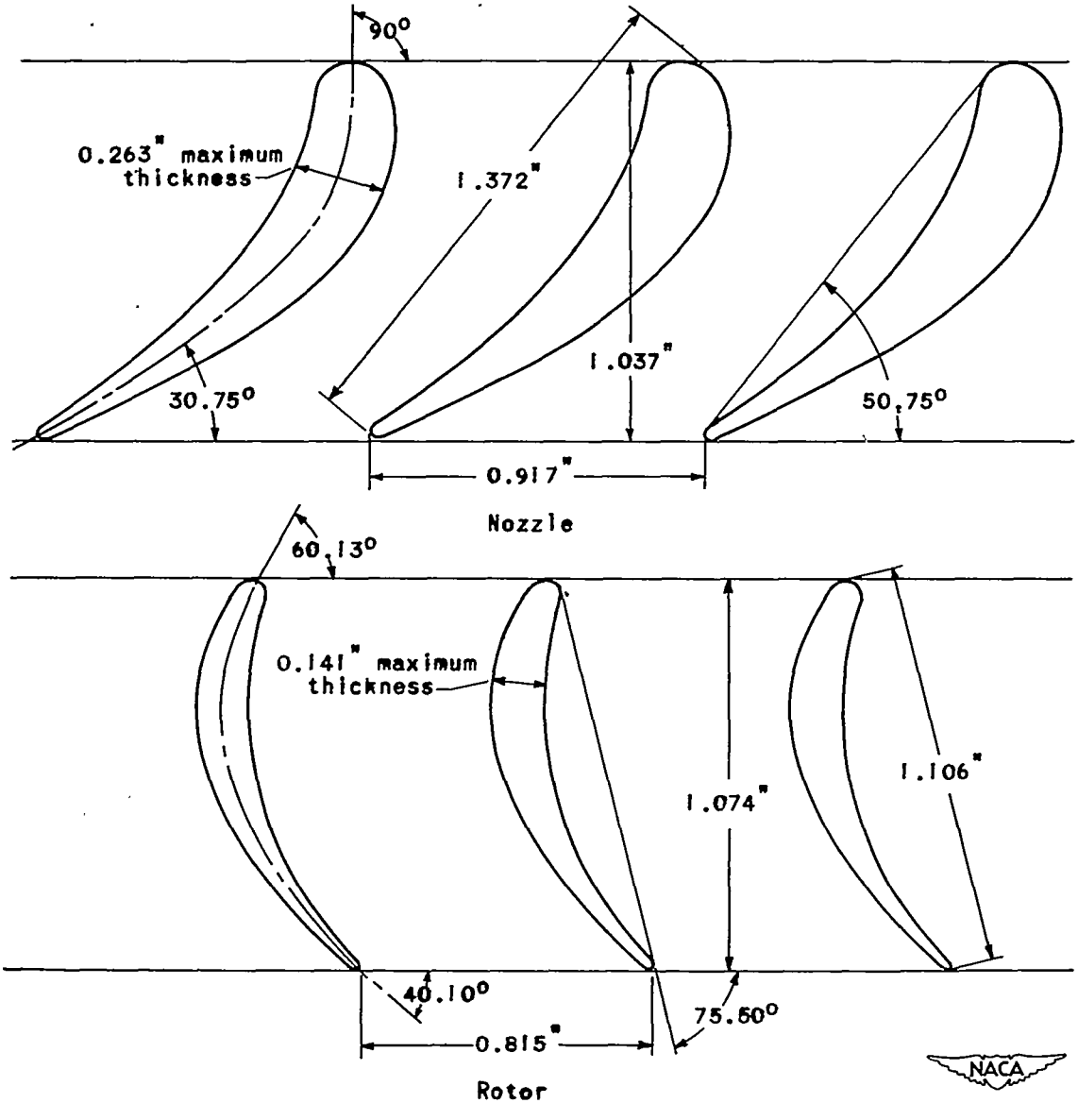

Figure 3. – Nozzle and rotor-blade detail at pitch line.

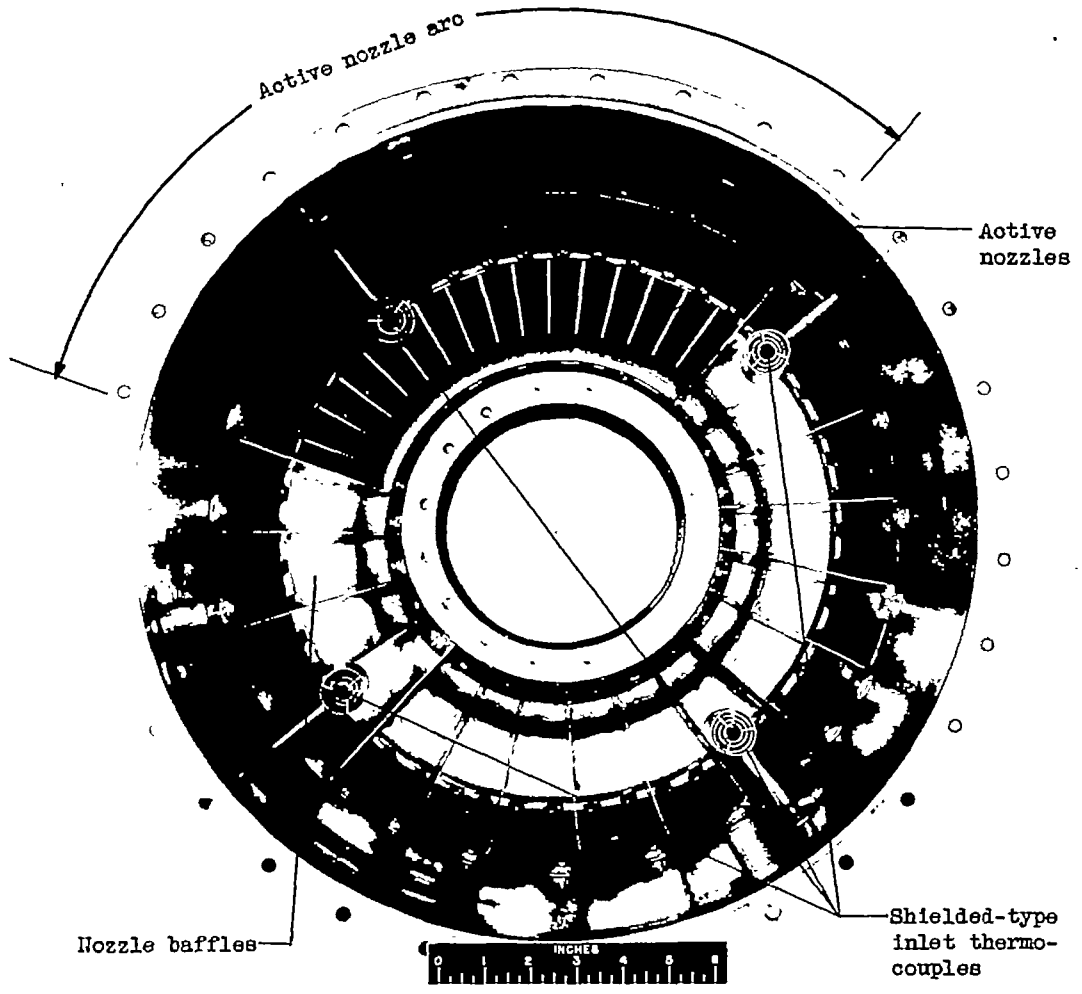

(a) Upstream view.

Figure 4. - Nozzle-inlet section of turbine with baffle segments installed for runs with gas admission over 120° of nozzle periphery.

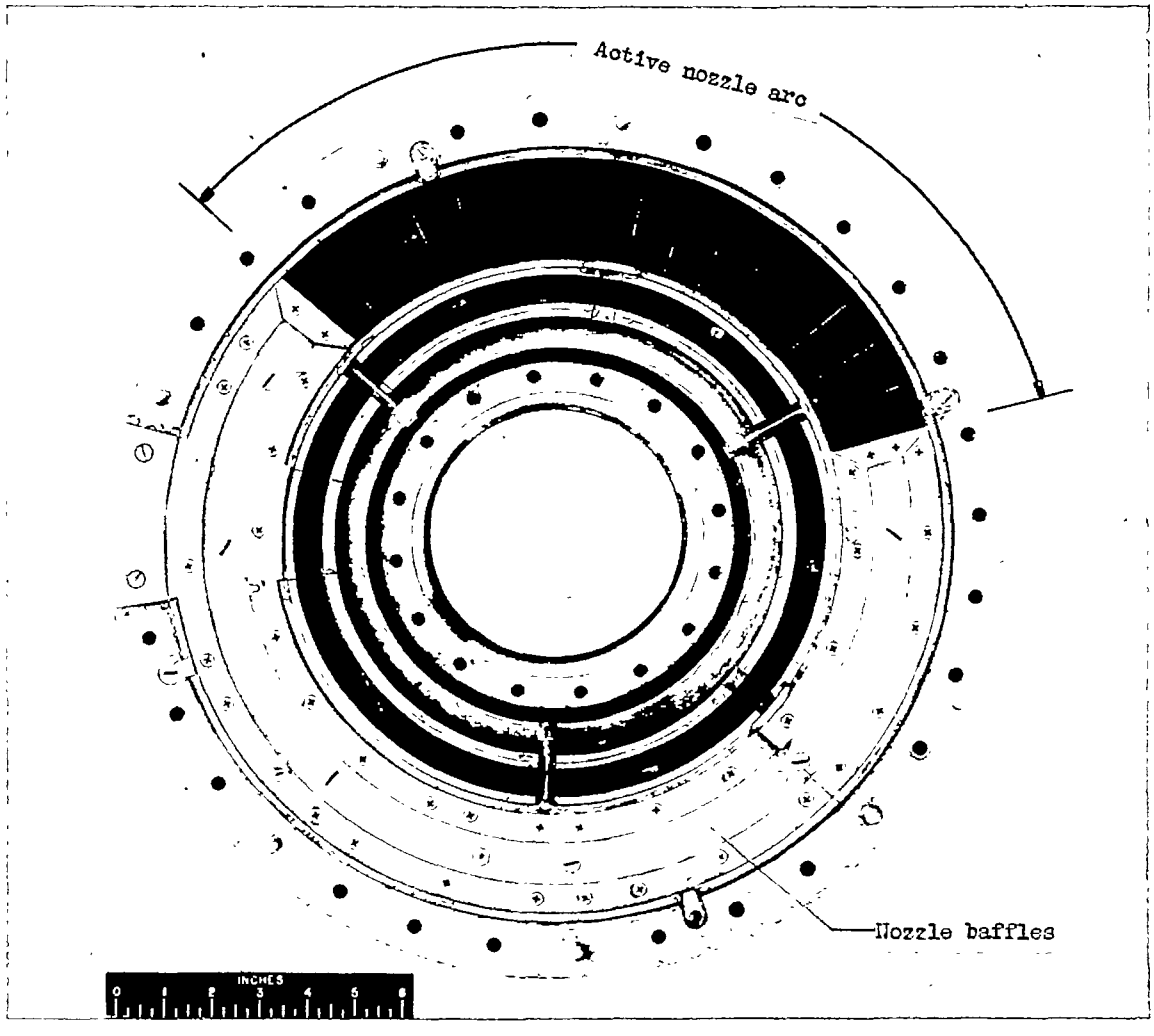

NACA
C-20548
1-29-48

(b) Downstream view.

Figure 4. - Concluded. Nozzle-inlet section of turbine with baffle segments installed for runs with gas admission over 120° of nozzle periphery.

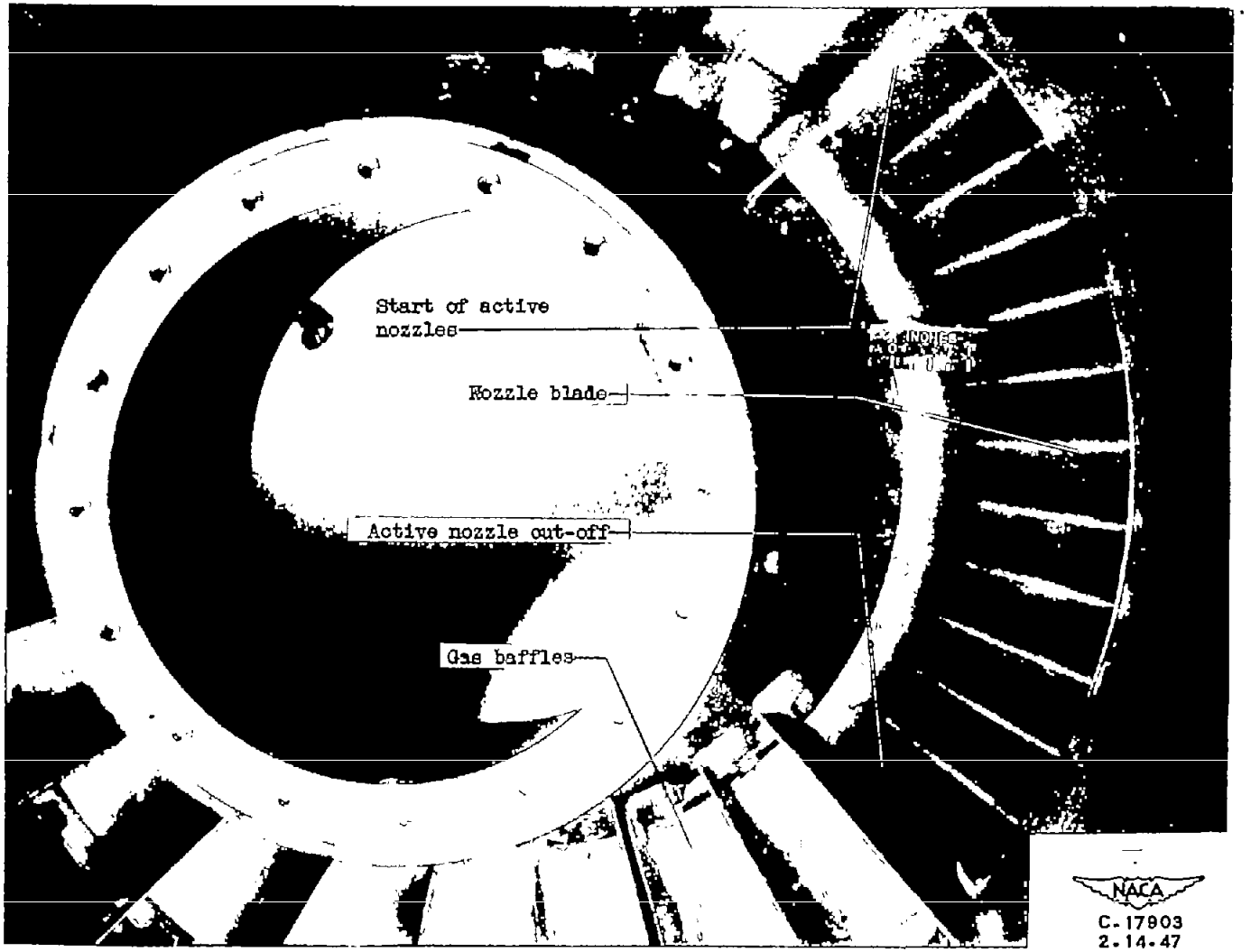

Figure 5. - Detailed view of nozzle inlet showing beginning and cut-off of active nozzle arc occurring along leading edges of nozzle blades.

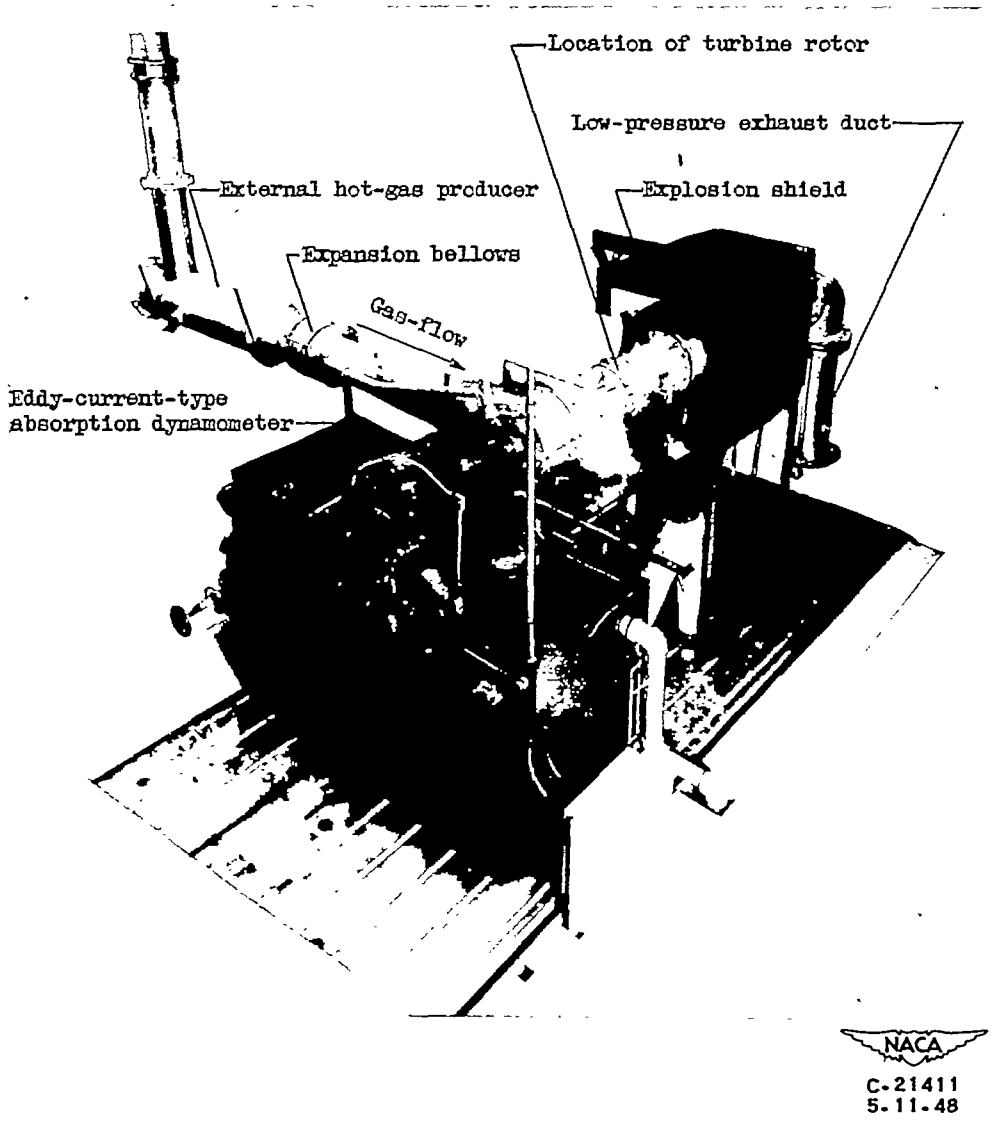

Figure 6. - Over-all test setup used for partial-admission investigation.

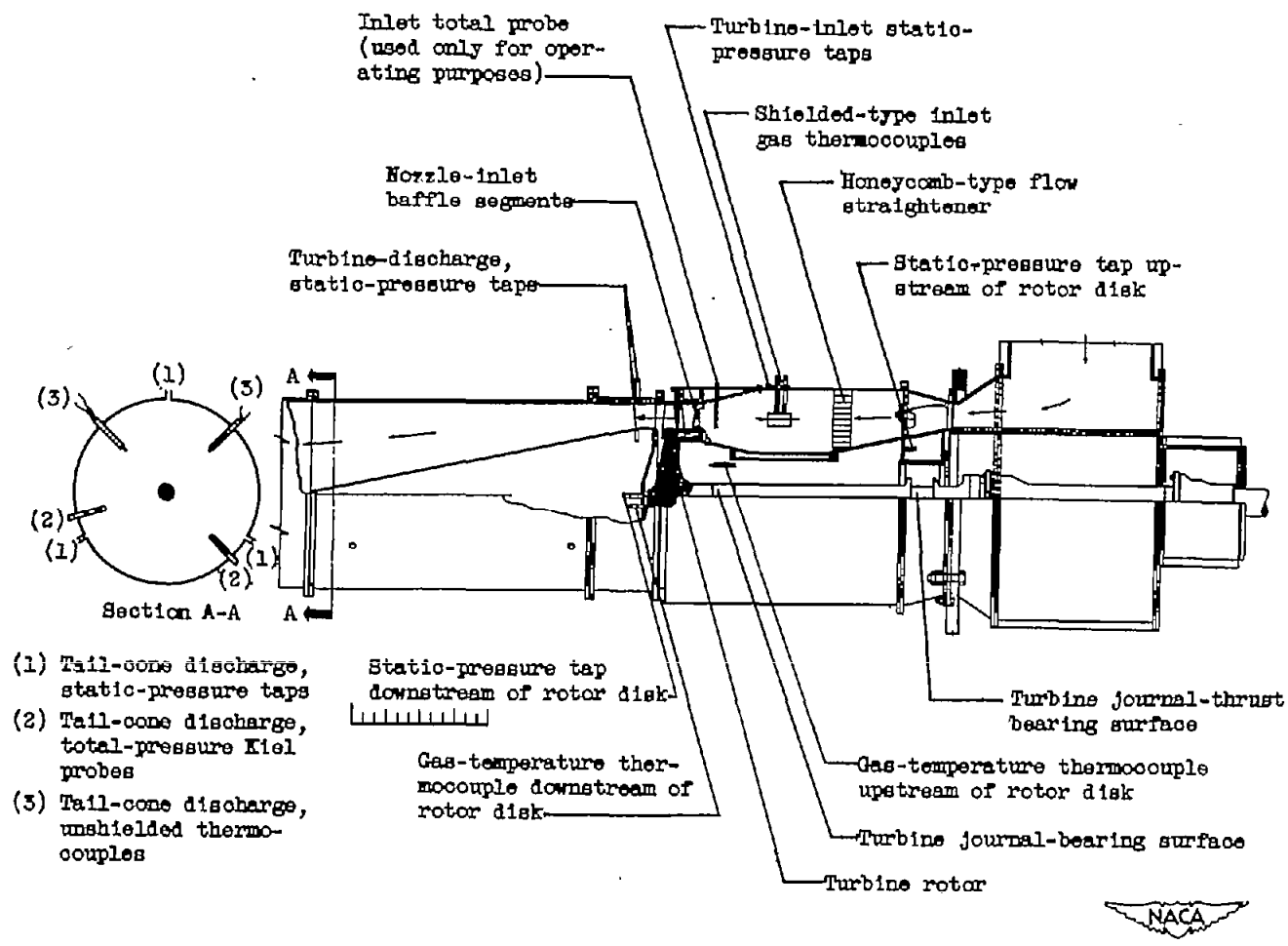

Figure 7. - Schematic plan of turbine assembly and instrumentation used in investigation of effect of partial admission on performance of gas turbine.

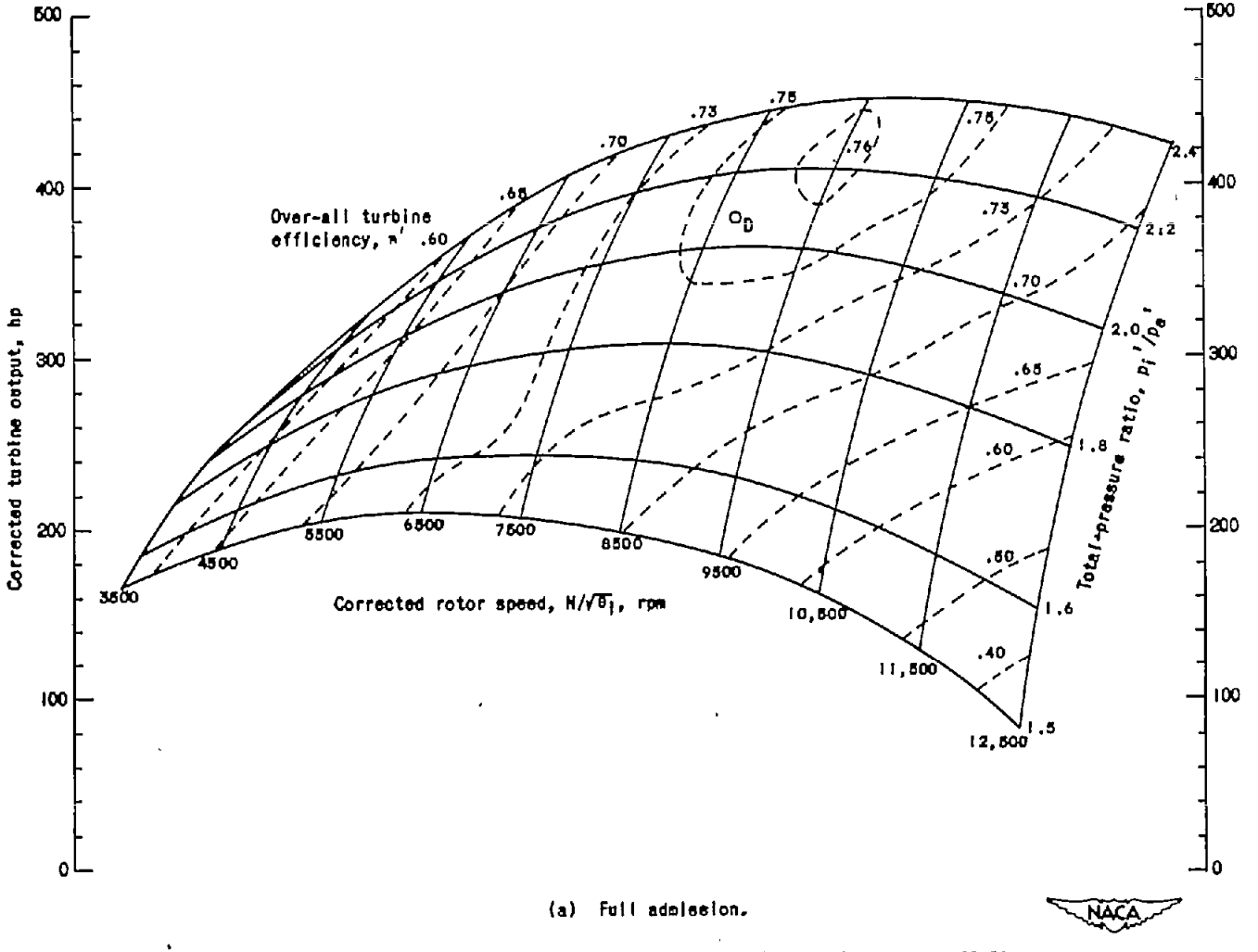

(a) Full admission.

Figure 8. - Performance characteristics of gas turbine. Corrected inlet total pressure, 29.92 inches mercury absolute; corrected inlet total temperature, 518.6° R; turbine rotor pitch-line diameter, 1.166 feet; flow area at turbine-inlet measuring station, 1.60 square feet; flow area at turbine-discharge measuring station (for full admission), 0.686 square foot. Turbine design operating point, D.

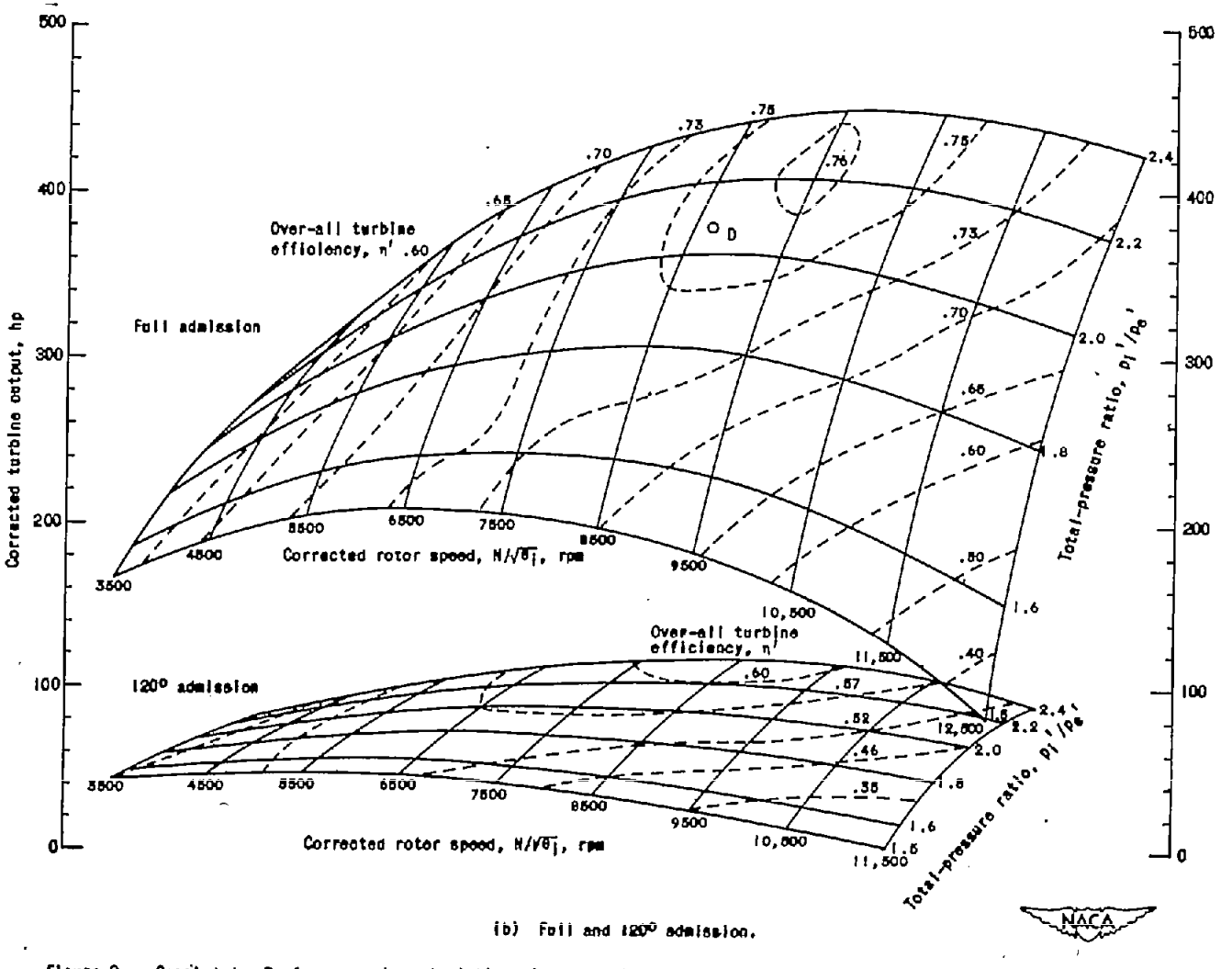

(b) Full and 120° admission.

Figure 8. - Concluded. Performance characteristics of gas turbine. Corrected inlet total pressure, 29.92 inches mercury absolute; corrected inlet total temperature, 518.6° R; turbine rotor pitch-line diameter, 1.166 feet; flow area at turbine-inlet measuring station, 1.60 square feet; flow area at turbine-discharge measuring station (for full admission), 0.686 square foot. Turbine design operating point, D.

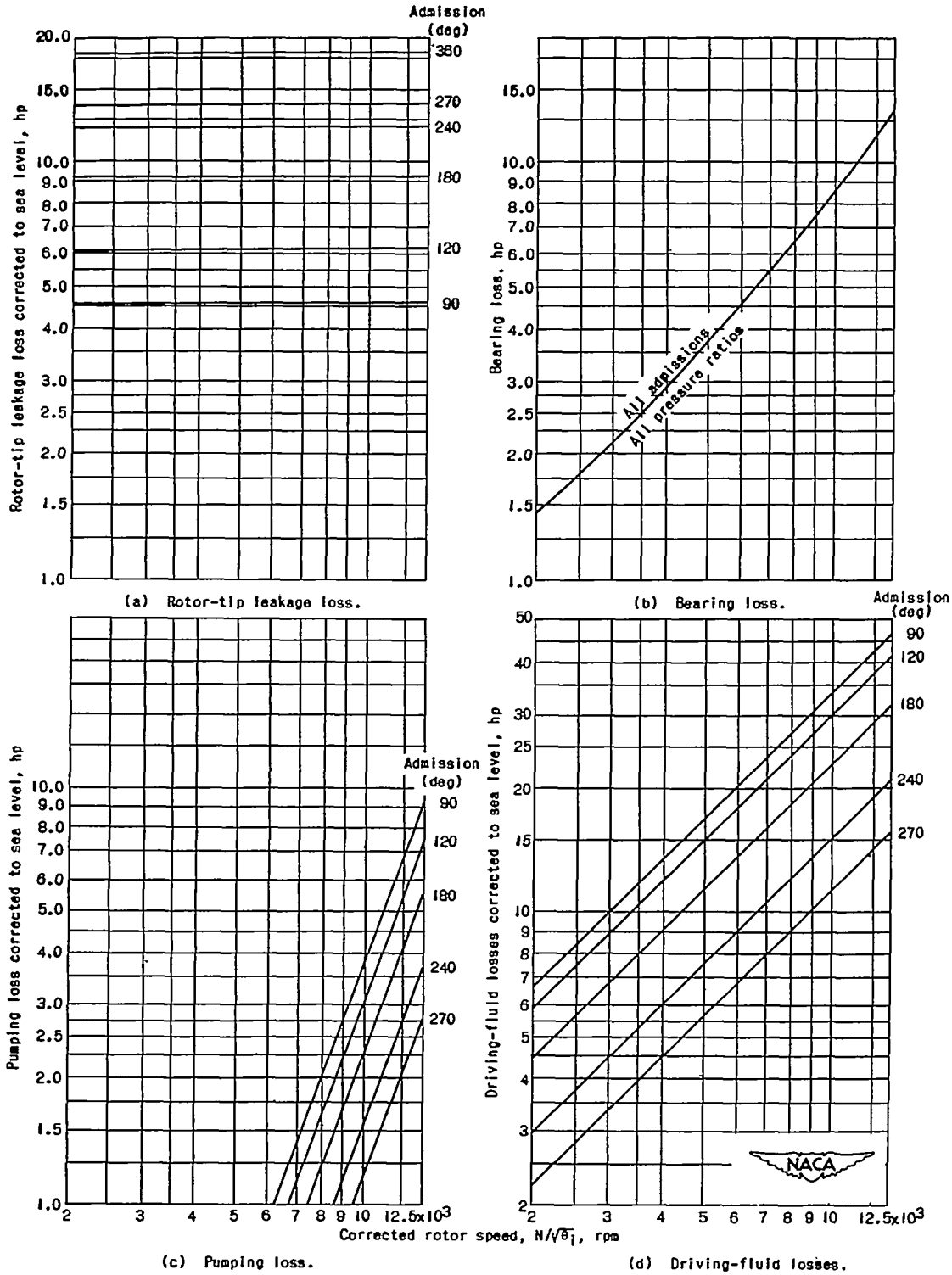

Figure 9. - Calculated and experimental losses for gas turbine operating at total-pressure ratio of 2.0 for full and partial admissions.

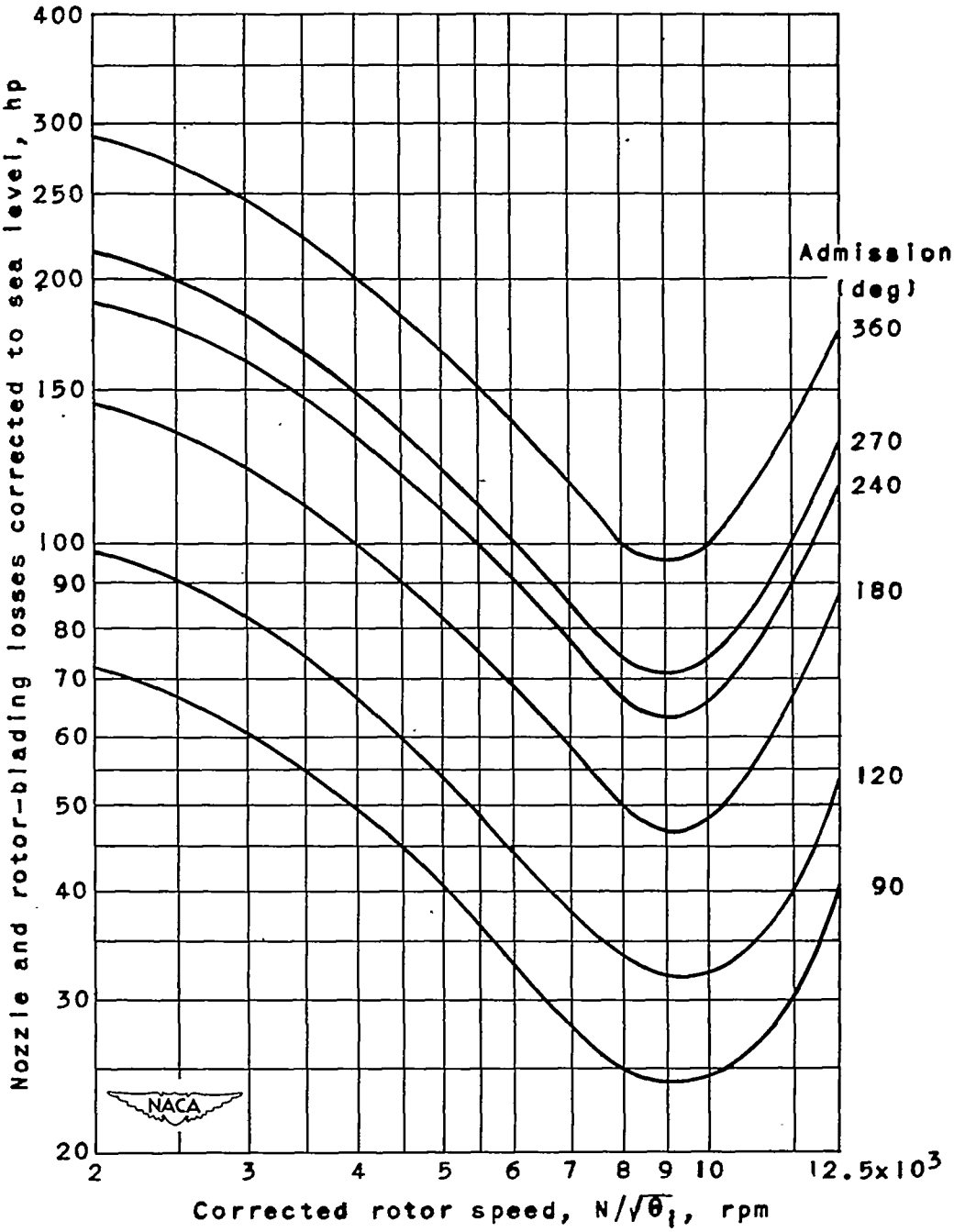

(e) Nozzle and rotor-blading losses.

Figure 9. – Concluded. Calculated and experimental losses for gas turbine operating at total-pressure ratio of 2.0 for full and partial admissions.

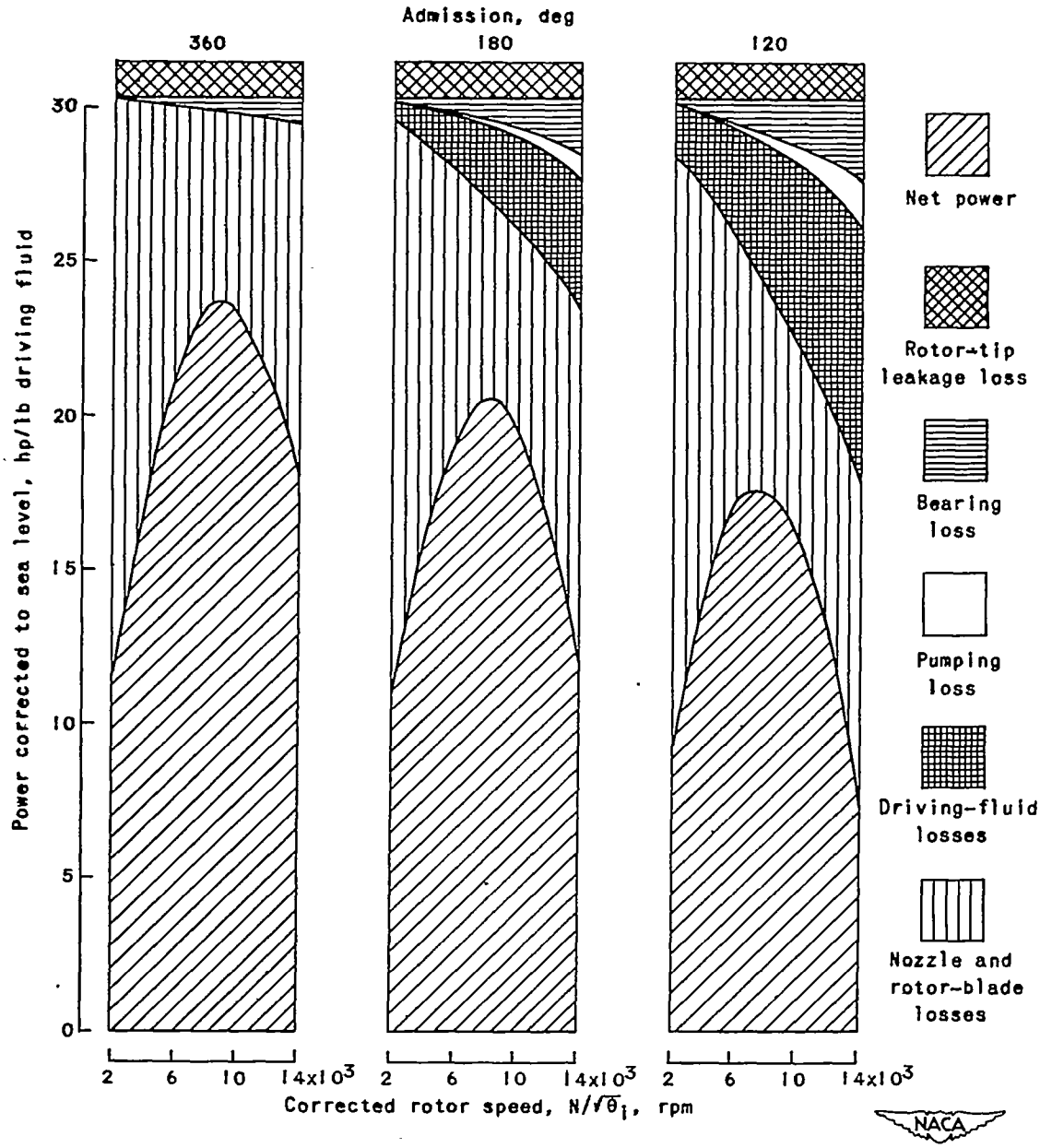

Figure 10. – Specific ideal power, specific net power, and applicable specific power losses for 360° (full), 180°, and 120° admissions. Total-pressure ratio, 2.0.

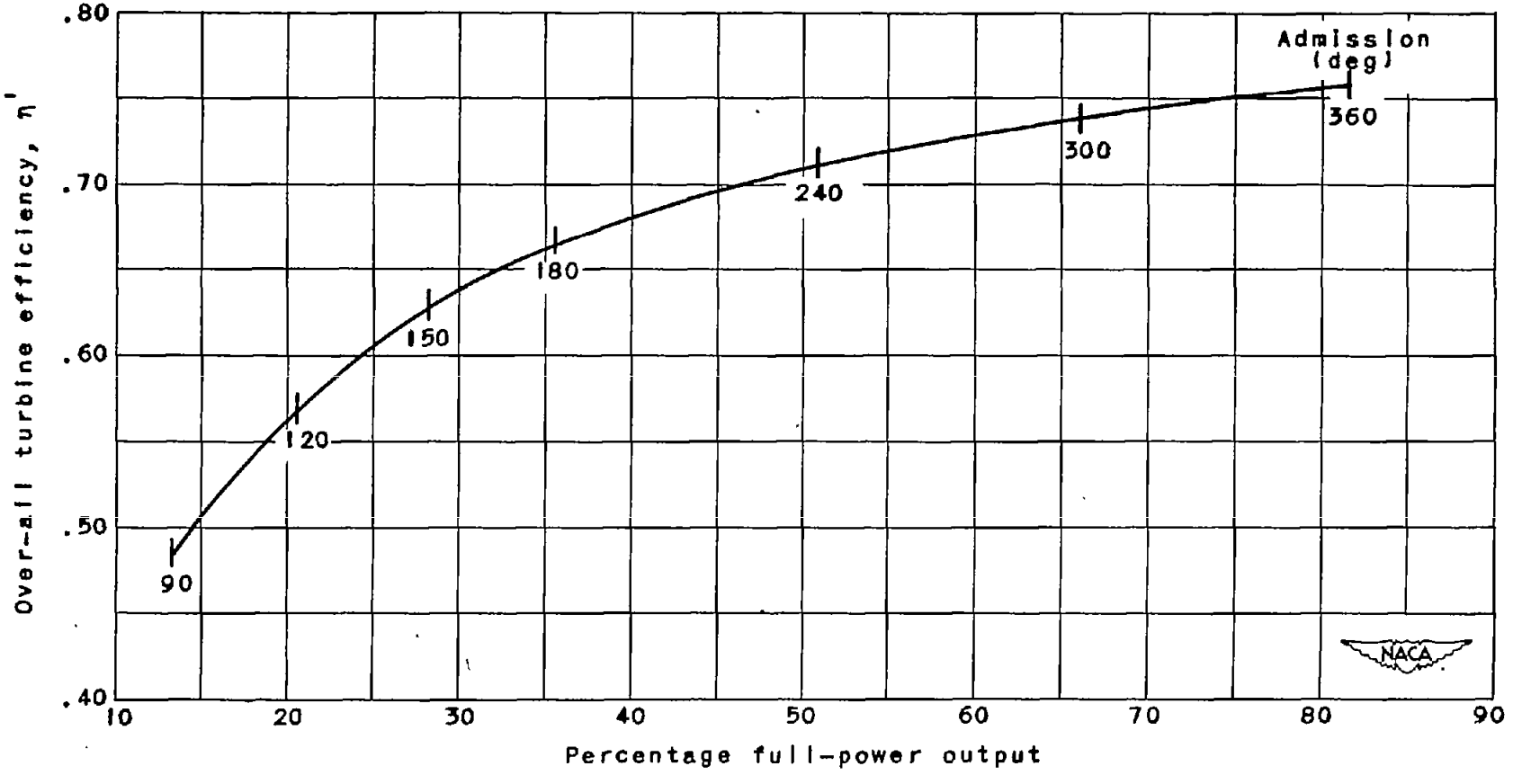

Figure 11. - Variation of over-all efficiency with power reduction by means of partial admission. Inlet total pressure, 45 inches mercury absolute; inlet total temperature, 800° R; corrected rotor speed, 8650 rpm; total-pressure ratio, 2.0.

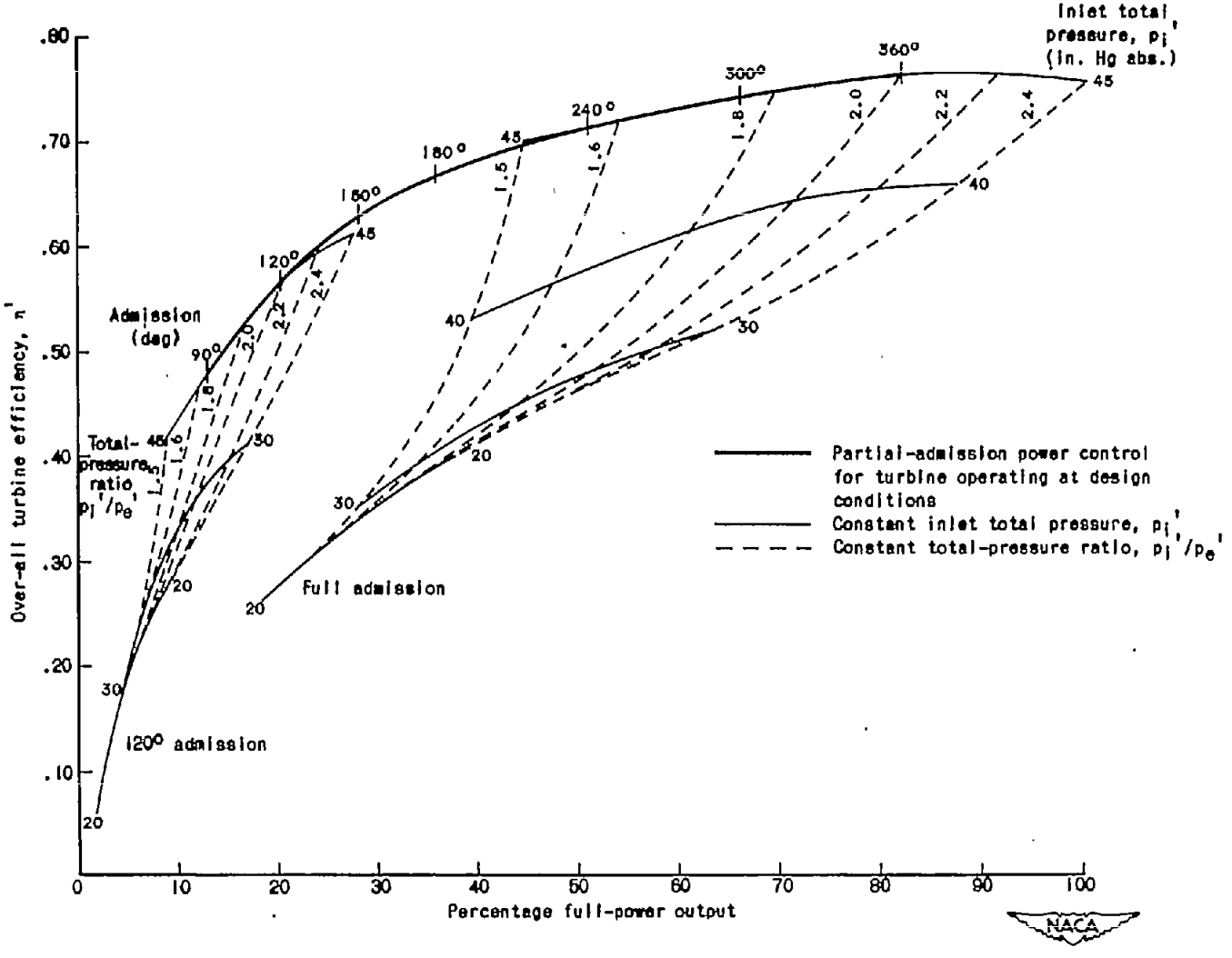

Figure 12. - Comparison of inlet pressure, pressure ratio, and active nozzle arc as gas-turbine-power-control parameters. Inlet total temperature, 800° R; corrected rotor speed, 8850 rpm.

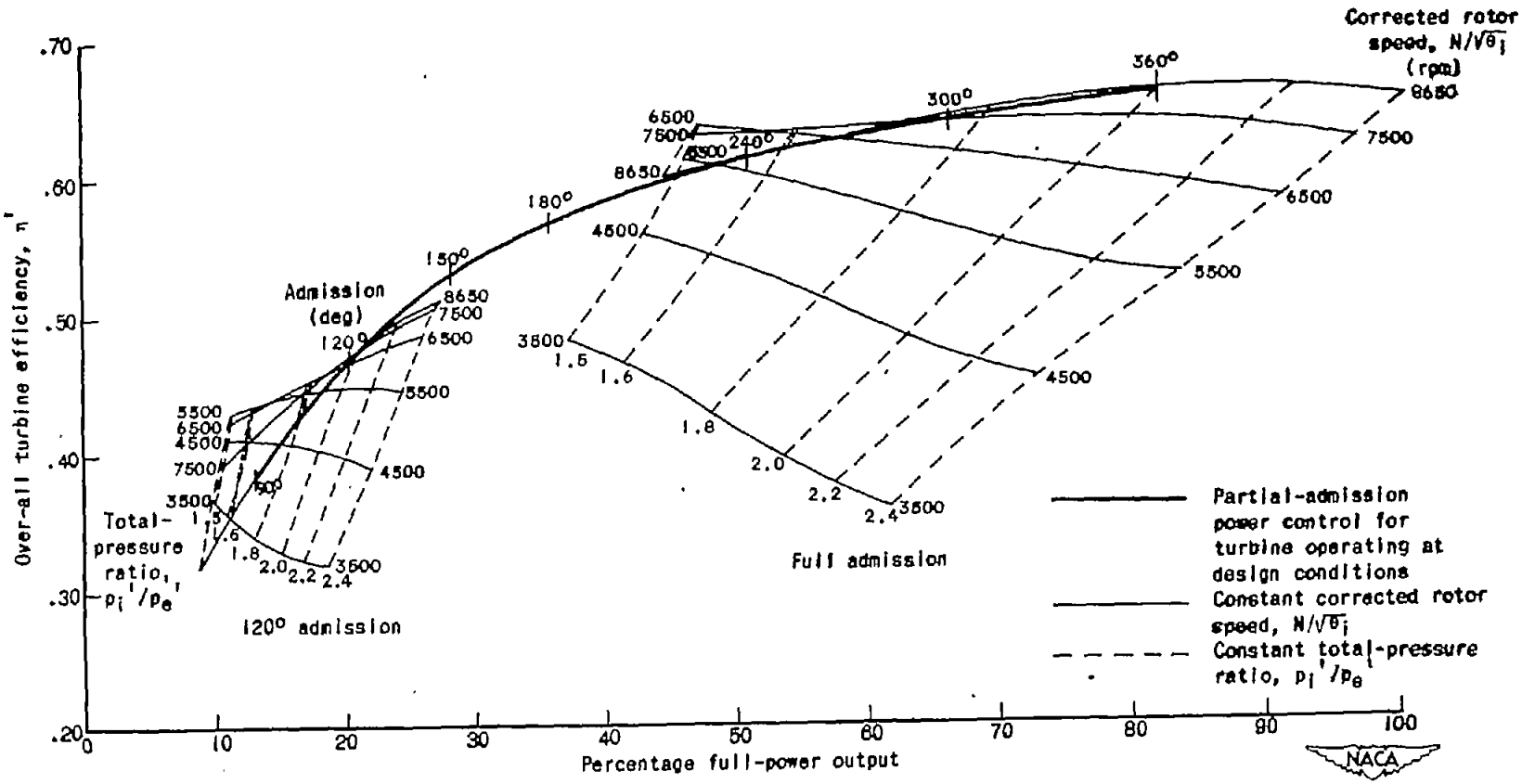

Figure 13. - Comparison of rotor speed, total-pressure ratio, and active nozzle arc as gas-turbine-power-control parameters. Inlet total temperature, 800° R; inlet total pressure, 45 inches mercury absolute.

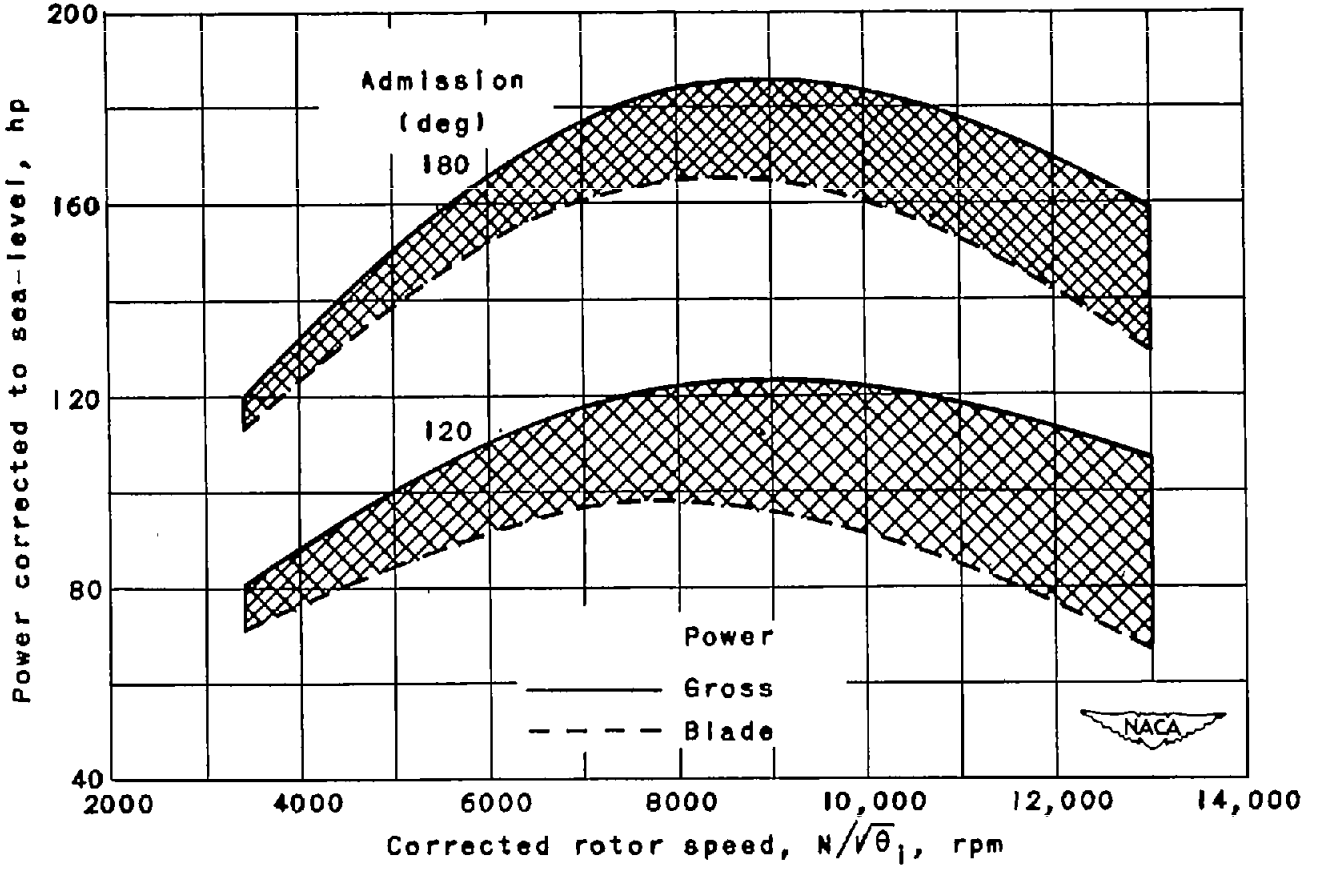

Figure 14. - Variation of driving-fluid losses (shaded areas obtained as difference between gross power and blade power) with rotor speed for 180° and 120° admission at total-pressure ratio of 2.0.